

EXPERIMENTAL INVESTIGATION OF PLASMA ACTIVATED
ETHANOL WATER SOLUTION

A Thesis

by

JOSEF SEBASTIAN

Submitted to the Office of Graduate and Professional Studies of
Texas A&M University
in partial fulfillment of the requirements for the degree of

MASTER OF SCIENCE

Chair of Committee,	David Staack
Committee Members,	Maria King
	Benjamin Wilhite
Head of Department,	Andreas A Polycarpou

May 2017

Major Subject: Mechanical Engineering

Copyright 2017 Josef Sebastian

ABSTRACT

Healthcare-associated infections (HAI) are infections that patients acquire while being treated at health care centers. Atmospheric pressure air plasmas created at or near room temperature are promising for treating HAI because of their strong anti-microbial effects, convenience and safety. Instead of applying plasma directly to biological substrates, chemical species from plasma can be used to activate liquids which in turn can be used to inactivate microorganisms. It has been known that plasma activated water (PAW) has strong anti-microbial properties, but recent studies show that plasma activated ethanol water (PAEW) solution has stronger sporicidal effects than PAW and results in 6 log reduction of bacterial endospores. Compared to PAW, little is known about chemical species in PAEW responsible for the sporicidal effects. The current work aims to identify species responsible for the significant sporicidal properties of PAEW compared to PAW.

A dielectric barrier discharge setup was used to activate the ethanol water solution with non-thermal ambient air plasma with this application in mind. The resulting plasma activated ethanol water solution is analyzed using various qualitative techniques like mass vs time trials, UV spectroscopy, FTIR spectroscopy and GCMS tests to identify the chemical species formed after plasma treatment. Quantitative analysis using various colorimetric and enzymatic assay tests was performed to quantify the chemical species formed in the ethanol water solution after plasma treatment. The spectroscopic tests revealed the presence of chemical species like nitrites, nitrates and

hydrogen peroxide in PAEW similar to that of PAW. New species with strong sporicidal activities like acetic acid and peracetic acid were also found in PAEW. These new species were later corroborated and quantified by well-known colorimetric and enzymatic assay tests specific for each species. The concentrations of acetic acid and peracetic acid were found to be in the 90 to 300 ppm range and 200 ppm range respectively after one minute of plasma treatment. Finally, a possible route for sporicidal action of peracetic acid is also discussed.

ACKNOWLEDGEMENTS

I am grateful to my advisor, Dr. David Staack, for presenting me with the opportunity to work under his guidance. I would like to thank my committee members Dr. Maria King and Dr. Benjamin Wilhite for their valuable suggestions.

I would also like to thank all the members of the plasma engineering and non-equilibrium processing laboratory, especially Kenneth Evans and Matthew Burnette for their invaluable support and assistance.

I would like to acknowledge the use of the TAMU Materials Characterization Facility and the support by Dr. Amanda Henkes for conducting various spectroscopic trials.

CONTRIBUTORS AND FUNDING SOURCES

This work was supervised by a thesis committee consisting of Dr. David Staack and Dr. Maria King of the Department of Mechanical Engineering and Dr. Benjamin Wilhite of the Department of Chemical Engineering.

All work for the thesis was completed independently by the student under the advisement of Dr. David Staack of the Department of Mechanical Engineering.

This work was made possible in part by EP Technologies LLC under TEES Project M1502474.

Its contents are solely the responsibility of the author and do not necessarily represent the official view of the sponsor.

NOMENCLATURE

PAW	Plasma Activated Water
PAEW	35% w/w Plasma Activated Ethanol Water Solution
UV-Vis	Ultraviolet- Visible
ATR	Attenuated Total Reflectance
FTIR	Fourier Transform Infrared Spectroscopy
GCMS	Gas Chromatography Mass Spectrometry
HAI	Healthcare Associated Infections

TABLE OF CONTENTS

	Page
ABSTRACT	ii
ACKNOWLEDGEMENTS	iv
CONTRIBUTORS AND FUNDING SOURCES.....	v
NOMENCLATURE.....	vi
TABLE OF CONTENTS	vii
LIST OF FIGURES.....	ix
LIST OF TABLES	xii
1. INTRODUCTION.....	1
1.1 Motivation	1
1.2 Plasma Activated Liquids	2
1.3 Ambient Air Plasma.....	3
1.4 Dielectric Barrier Discharge.....	6
1.5 Liquid Phase Chemistry	7
2. EXPERIMENTAL INVESTIGATION OVERVIEW	9
2.1 Objective	9
2.2 Experimental Setup	11
2.3 Proposed Tasks.....	13
3. MASS AND ENERGY CALCULATIONS	15
3.1 Mass vs Time Trials	15
3.2 Variation of Input Parameters	17
3.2.1 Variation with Power	18
3.2.2 Variation with Activation Time	19
3.2.3 Variation with Concentration	20
3.2.4 Variation with Initial Temperature	22
3.3 pH Test	23
3.4 pH Test Calculations	24

3.5 Discharge V-I Characteristics	25
3.6 Energy Estimates of Species Generation.....	29
4. QUALITATIVE ANALYSIS	30
4.1 UV-Vis-NIR Spectroscopy.....	30
4.1.1 UV-Vis-NIR Spectrum for 190- 3300 nm.....	31
4.1.2 UV Spectrum for 200-400 nm.....	33
4.2 ATR-FTIR Spectroscopy	37
4.3 GCMS.....	39
5. QUANTITATIVE ANALYSIS	47
5.1 Detection of Hydrogen Peroxide.....	47
5.2 Detection of Nitrites and Nitrates.....	50
5.3 Detection of Acetic Acid.....	52
5.4 Detection of Peracetic Acid.....	55
6. SPORICIDAL ACTION OF PLASMA ACTIVATED ETHANOL WATER SOLUTION.....	57
7. CONCLUSIONS AND FUTURE WORK	60
7.1 Conclusion.....	60
7.2 Summary of Results	60
7.2.1 Mass vs Time Results.....	60
7.2.2 pH Trials.....	61
7.2.3 Qualitative Analysis	61
7.2.4 Quantitative Analysis	63
7.2.5 Sporicidal Action.....	63
7.3 Future Work	64
REFERENCES.....	65
APPENDIX A	72
APPENDIX B	77
APPENDIX C	79
APPENDIX D	81
APPENDIX E.....	84

LIST OF FIGURES

	Page
Figure 1: Common dielectric barrier configurations. a) Planar dielectric barrier discharge and b) Annular dielectric barrier discharge	6
Figure 2: Possible reaction products in PAW solutions.....	8
Figure 3: a) Experimental results of tests done at EP technologies LLC. b) Sporicidal effects of untreated water, untreated ethanol, PAW and PAEW	10
Figure 4: a) Experimental setup for DBD discharge including the power supply, electrode arms, electrode and teflon holder. b) A zoomed in view of the electrode and teflon holder while the system is on is also shown.	12
Figure 5: Schematic of the experimental setup (not to scale).	13
Figure 6: The difference in normalized evaporated mass between treated and untreated ethanol-water mixture	16
Figure 7: Mass vs time trials for 35 % untreated and treated samples at different powers.....	19
Figure 8: Mass vs time trials for 35 % untreated and treated samples for different activation times	20
Figure 9: Mass vs time trials for untreated and treated samples for different concentrations	21
Figure 10: Mass vs time trials for 35 % untreated and treated samples for different temperatures.....	23
Figure 11: pH test results for both DI water and 35% ethanol water before and after plasma treatments	24
Figure 12: Discharge VI characteristics of the experimental setup in the case of plasma activation of DI water and ethanol water samples	26
Figure 13: Instantaneous power plots of setup using DI water and ethanol water solution.	28
Figure 14: UV-Vis- NIR spectrophotometer at MCF.	30

Figure 15: Wavelength dependent absorbance for plasma treated samples of ethanol water mixtures in the 190- 3300 nm range. A zoomed in plot of fingerprint region 2500-3500 nm is also shown.	32
Figure 16: UV Spectrum of DI water and 35% w/w ethanol water solution before and after plasma treatment.....	34
Figure 17: Time dependent UV spectrum of 35% ethanol water mixture after plasma treatment	35
Figure 18: UV spectrum of vapors coming out of 35% ethanol water mixture after plasma treatment.....	36
Figure 19: The Diamond tipped ATR stage and Thermo Nicolet 380 FTIR spectrometer.....	38
Figure 20: FTIR absorption spectra of the untreated and plasma treated samples of 35% w/w ethanol-water solution	39
Figure 21: GCMS setup at Chemistry Mass Spectrometry Facility.....	40
Figure 22: GCMS spectra of plasma treated DI water solution. The identified species are labelled as shown.	41
Figure 23: Mass spectra at same elution time ($t = 3.85$ sec) for ethanol water mixture before and after plasma treatment.....	42
Figure 24: Comparison of mass spectra of PAEW with individual spectra of ethanol, water and acetic acid.....	43
Figure 25: Mass spectra at same elution time ($t = 3.85$ sec) for ethanol water mixture before and after treatment for different activation times	44
Figure 26: Hydrogen peroxide detection for PAEW using Chemtrix VACUettes visual high range kits.....	49
Figure 27: Hydrogen peroxide detection using Lamotte test kit. The test kit produced similar test results as the Chemtrix test kit.....	50
Figure 28: Nitrite and nitrate detection using Seachem multitest nitrite and nitrate test kit	51
Figure 29: Nitrite and nitrate detection using Seachem multitest nitrite and nitrate test kit for different post discharge times for PAEW	52

Figure 30: Experimental absorption curve of the decrease in the absorbance of NADH with time.	55
Figure 31: Peracetic acid detection using Lamotte test kit using DPD method	56
Figure 32: Endospore structure of the spore forming bacteria.	58
Figure 33: Possible reactive species in PAEW.	62

LIST OF TABLES

	Page
Table 1: Statistical analysis results of mass vs time trials.....	17
Table 2: Spectrophotometric results of PAEW	54
Table 3: Quantitative analysis results.....	63

1. INTRODUCTION

1.1 Motivation

Healthcare-associated infections (HAI) are infections that patients acquire while being treated at health care centers. According to a study conducted in 2002, about 1.7 million infections occur annually resulting in 99,000 deaths which make it one of the most complicated problems associated with modern day health care [1]. The costs associated with HAI are estimated to be around \$9.8 billion each year [2]. There is a real need for some novel techniques for antimicrobial disinfection in health care institutions.

Non-equilibrium air plasmas at atmospheric pressures have gained a prominent role in plasma biotechnology due to its ease of production and use. Non-thermal ambient air plasmas are of increasing interest for biological and medical applications in the emerging field of plasma biotechnology also known as plasma medicine. The use of non-thermal atmospheric air plasma to inactivate harmful microorganisms is called plasma disinfection. Reactive oxygen species (ROS) like peroxides, superoxides, hydroxyl radical and singlet oxygen are produced by non-thermal plasma [3]. Oxidative defense mechanisms involving these ROS have an important role in innate immune system [4].

Non-thermal plasma technology has been used to activate various liquids which result in a strong biocidal agent commonly known as plasma activated liquids. Recent studies have been conducted to investigate the antimicrobial activity of plasma activated

water(PAW) and saline solutions[3]. This study presents a novel plasma activated liquid that is more effective as an antimicrobial agent compared to plasma activated water.

1.2 Plasma Activated Liquids

Cold atmospheric pressure plasmas have been used in a wide variety of fields ranging from water purification to nanoparticle synthesis [5, 6] Over the last decade, considerable research has been done on the application of non-thermal atmospheric pressure plasmas in the field of biomedicine [3]. Most of the research in plasma medicine is focused on applying plasma directly to tissues, biological fluids and material surfaces [7].

Non-thermal plasmas can be directly applied to cells to produce anti-microbial effects or the reactive species from plasmas can be transferred to a liquid medium which can be subsequently applied to a biological system or cells. The liquids activated by non-thermal plasma that results in anti-bacterial effects are referred to as plasma activated liquids. The indirect treatment by plasma activated liquids has many benefits compared to direct application of plasma to surfaces as the surface is not in direct contact with plasmas and while also being easier to apply than direct treatment.

Ambient air plasmas contain various reactive oxygen species like hydroxyl radicals(OH), superoxide anion(O_2^-), reactive nitrogen species like nitric oxide (NO) and many more species which are known to have various biological applications [8]. However, these species have short lifetimes and do not penetrate deep into the liquid

media. On the other hand, they can interact with the liquid to generate relatively stable long-lived species inside the volume of the liquid. The main reactive species formed after plasma treatment of water were found to be long lived reactive oxygen species (ROS) like hydrogen peroxide (H_2O_2) and long lived reactive nitrogen species (RONS) like nitrite (NO_2^-) and nitrate (NO_3^-) [9]. It has also been experimentally verified that the above species might not be the only species responsible for antimicrobial action [10]. The available literature in the field of plasma activated liquids is for the plasma activation of traditional liquids like water and saline solutions [3]. The focus of this study is to identify the chemical species responsible for the antimicrobial action of plasma activated ethanol-water which is a nontraditional solution.

1.3 Ambient Air Plasma

Plasmas make up more than 99% of visible matter in the universe. They consist of positive ions, electrons, negative ions and neutral particles. Plasma is commonly referred to as the fourth state of matter. When a solid is heated, atoms or molecules gain enough energy and melt into liquid. When this liquid is heated, particles in a liquid gain enough energy and vaporize into a gas. When energy is applied to this gas through electric field, the electrons that escape from the atoms or molecules collide with other atoms to produce more ions and electrons [11]. The higher number of electrons and ions change the property of the gas and we can refer to it as ionized gas or plasma. The most common process in plasma formation is ionization which is the conversion of neutral

atoms or molecules into electrons and positive ions. The plasma is quasi-neutral i.e. the number of electrons is equal to the number of positive ions.

Naturally occurring electrons obtain energy from electric field because of their low mass and high mobility and the energy is used for ionization, excitation, dissociation and other chemical processes. The energy transfer from electrons to the heavy particles occurs through ionization, excitation, dissociation of molecules and elastic collisions. In most plasmas under consideration, the mean electron energy is in the range of 1-5 eV [7]. In the case of molecular gases vibrational excitation is normally dominant in these range of electron temperatures. In the case of atomic gases energy transfer from electrons to heavy particles is mainly dominated by electronic excitation and ionization. The combination of these processes leads to the formation of ions, electrons, neutrals and excited species which constitute the plasma.

Plasmas are divided into two categories: thermal (hot plasmas) and non-thermal (cold plasmas). Thermal plasmas are characterized by equal gas and electron temperatures or energies. Non-thermal plasmas are characterized by electrons with much greater energy than ions and neutral species. In non-thermal plasmas, electron temperatures are much higher than gas temperatures which remain almost unchanged. Because the different components exist at different temperatures, such plasmas are said to be non-equilibrium. In recent years, cold atmospheric pressure plasma sources have been developed that, in principle, provide the possibility to extend plasma treatment to living tissue [12].

Chemical species formed in the air plasma region due to the combination of above processes are atomic nitrogen (N) and oxygen (O), excited states including singlet-delta oxygen ($O_2(a^1\Delta_g)$) and vibrationally excited nitrogen ($N_2(v)^*$), ions including oxygen molecular ion (O_2^+) nitrogen molecular ion (N_2^+), and high-energy photons in the UVB–UVA range[3, 13-15]. Other neutral and ionic species are present in plasma because of the association and dissociation products of the species mentioned above.

Industrially, the most important application of non-thermal plasmas is the low-pressure processing of materials, often for microelectronics and semiconductor fabrication [16]. The high pressure conditions raises the gas temperature as the collision frequency increases which increases the energy transfer from electrons to gas molecules [11]. However, many devices have been developed to obtain non-thermal atmospheric pressure (high pressure) plasma at ambient conditions have been developed including DBD, gliding arc, corona, and plasma jet[17-21]. These devices work on the principle that T_e (electron temperature) $\gg T_g$ (gas temperature) if one or more of the following criteria are met [11].

- a) Preventing thermalization or equilibrium by pulsing the plasma
- b) Using the circuit to limit current by increasing the electric field using sharp discharges as in corona discharges or reducing the electron density or current by introducing dielectric barriers
- d) Improving the heat transfer

1.4 Dielectric Barrier Discharge

The Dielectric Barrier Discharge (DBD) works on the principle that introducing a dielectric between the metal electrode and the plasma can be used to reduce the current thereby maintain $T_e \gg T_g$ for practical applications. The displacement current through the dielectric causes the continuity of the current in the circuit so in this case discharge has to be driven by AC or pulsed voltage excitation [22]. In the case of DBD at least one of the electrodes are covered by dielectric barrier and DBD's have been generated in parallel-plate or coaxial cylindrical reactor geometries. Common dielectric barrier configurations are shown in Figure 1 [23].

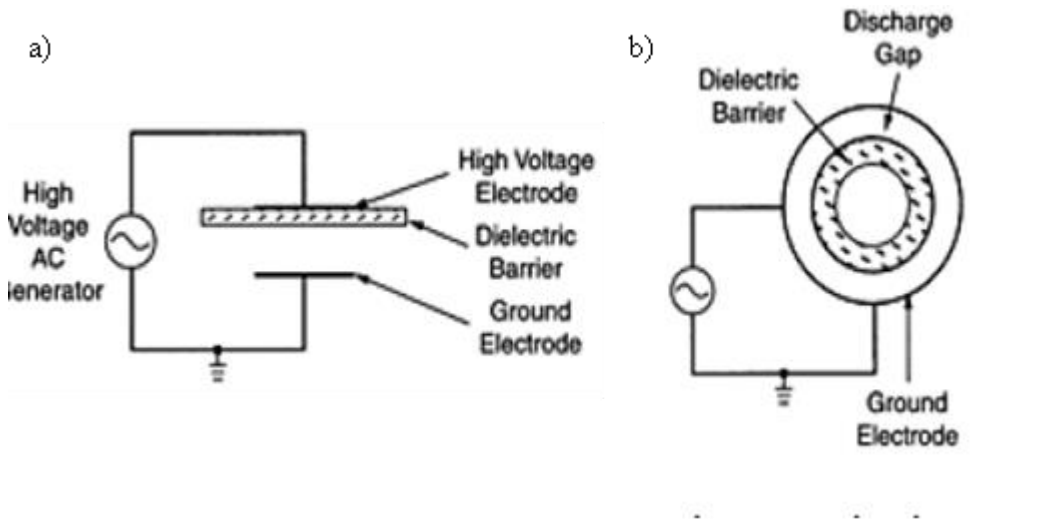


Figure 1: Common dielectric barrier configurations. a) Planar dielectric barrier discharge and b) Annular dielectric barrier discharge

The experiments at PEDL were conducted in parallel plate configuration similar to Figure 1a with one dielectric and a gas gap. Charge accumulates on the surface of the

dielectric layer until the breakdown potential of the surrounding gaseous medium is reached. Then, transient filaments form between the dielectric layer and the grounded electrode, which is where ionization occurs and the plasma itself is formed [11]. The grounded electrode is the stainless-steel mesh which allows for the chemically active species in the plasma to interact with the ethanol water solution kept below the ground electrode.

1.5 Liquid Phase Chemistry

The chemical mechanism of disinfection is somewhat understood for aqueous systems including water and saline systems and less well characterized for water-ethanol systems. The list of reactive species that are produced after plasma activation varies significantly depending on the study, the plasma source, and the operating parameters. It has been established that nitric acid/nitrate ($\text{HNO}_3/\text{NO}_3^-$), nitrous acid/nitrite ($\text{HNO}_2/\text{NO}_2^-$), and hydrogen peroxide are among the species produced after plasma treatment of water [3, 24, 25]. The complex chemistry of air plasmas and the associated plasma-water chemistry are areas of active research and further investigation will be needed to fully understand these systems.

Also peroxynitrous acid/peroxynitrite ($\text{HONOO}/\text{ONOO}^-$) was found to be produced in water after plasma activation [26]. A common method to generate peroxynitrite is to mix aqueous solutions of acidified H_2O_2 with NO_2^- [27]. Both of these species are known to be created in air plasma, so it seems likely that ONOO^- (or

ONOOH) is also generated in water exposed to air plasma[26]. Recently, peroxyntiric acid/peroxyntirate ($\text{HO}_2\text{NOO}/\text{O}_2\text{NOO}^-$) has been identified as a potentially important species responsible for the antimicrobial action of plasma activated water [28]. The possible reactive species in PAW are summarized in Figure 2 [29].

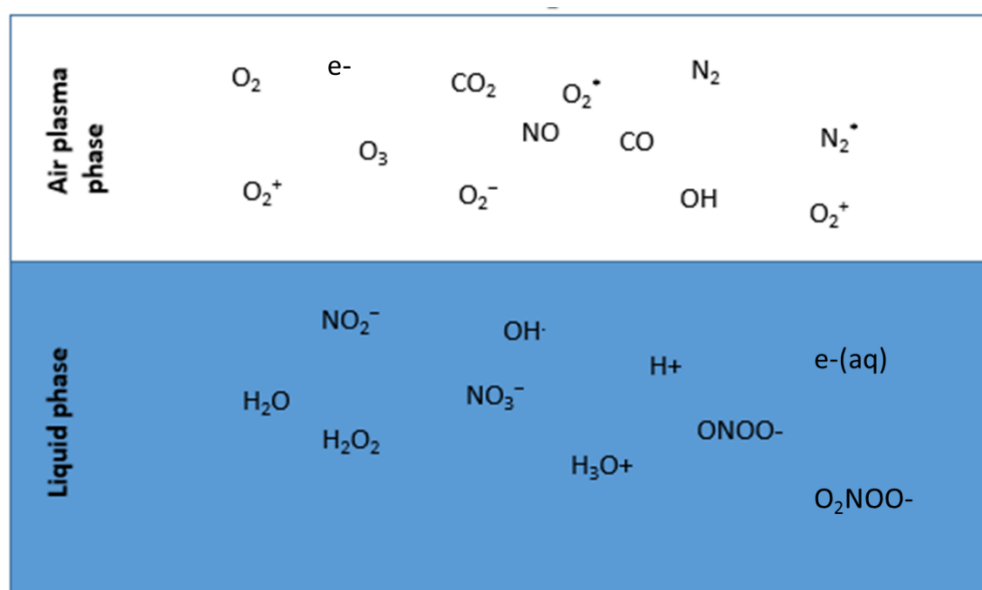


Figure 2: Possible reaction products in PAW solutions.

The research in recent years was to identify the reactive species responsible for the antimicrobial activity of PAW solution. The research to identify the plasma activation of ethanol water mixture (PAEW) is a novel attempt and will be discussed in the coming chapters.

2 EXPERIMENTAL INVESTIGATION OVERVIEW

2.1 Objective

The initial research conducted at EP technologies LLC on plasma activated liquids provided some promising results. Researchers have experimentally found that plasma activation of ethanol-water solution at a particular set of initial conditions and using a dielectric barrier discharge (DBD) setup resulted in increased logarithmic reduction of bacterial spores compared to plasma activation of water as shown in Figure 3a. The bacterial spores that was tested were *Clostridium difficile* which is a common pathogen found in healthcare institutions. On the basis of a recent study, estimate of the annual burden of *Clostridium difficile* infections in the United States is 453,000 cases per year with 29,300 associated deaths [30]. Alcohols like ethanol lack activity against spores and use of alcohol sanitizers doesn't reduce levels of spores on hands [31]. The 35% ethanol water solution was found to be the most effective concentration among the different concentrations tested and resulted in six-fold logarithmic reduction in concentration of spores. The objective of this study is to identify the chemical species responsible for this sporicidal activity and quantify the concentration of the species. A summary of the sporicidal activity of untreated ethanol, untreated water, plasma treated water (PAW) and plasma treated 35% w/w ethanol water (PAEW) solution on *Clostridium difficile* is shown in Figure 3b. The experiments at PEDL are conducted

with an identical set up and at the exact initial conditions as the tests conducted at EP technologies LLC.

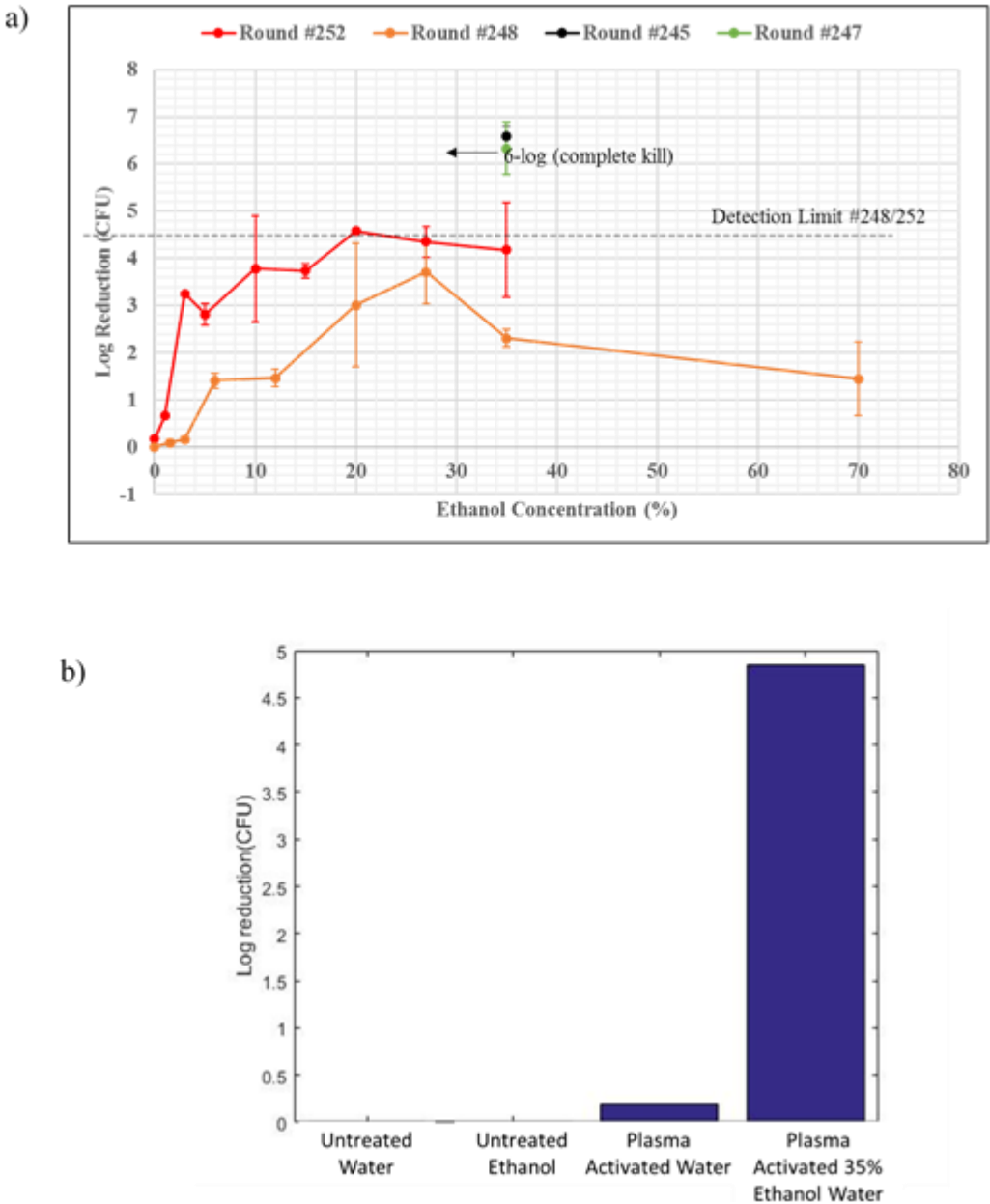


Figure 3: a) Experimental results of tests done at EP technologies LLC. b) Sporicidal effects of untreated water, untreated ethanol, PAW and PAEW. The PAEW was found to be more effective in killing bacterial spores compared to plasma activated water.

2.2 Experimental Setup

The experimental setup in Plasma Engineering and Non-Equilibrium Processing Laboratory consists of an AC power source that generates air plasma by a dielectric barrier discharge system as shown in Figure 4. This specific setup was supplied by EP technologies LLC to exactly duplicate their conditions. The electrode is connected using an insulated high voltage (HV) cable from a power supply (Amazing1 PVM500). The system is operated at 26 kHz and 13 W as monitored by fluke multimeter and digital power meter (Belkin Kill A Watt). The HV electrode is attached to a quartz plate of thickness 1 mm with silicone RTV. A stainless steel mesh electrode used as ground was fixed at a 1 mm gap from the quartz plate with a spacer. The gap distance between the grounding electrode and the Teflon holder was fixed at 1 mm. A 35% w/w solution of 200 proof ethanol and distilled water was prepared during each trial and it was held under the plasma using a Teflon holder. A schematic of the experimental setup is also shown in Figure 5.

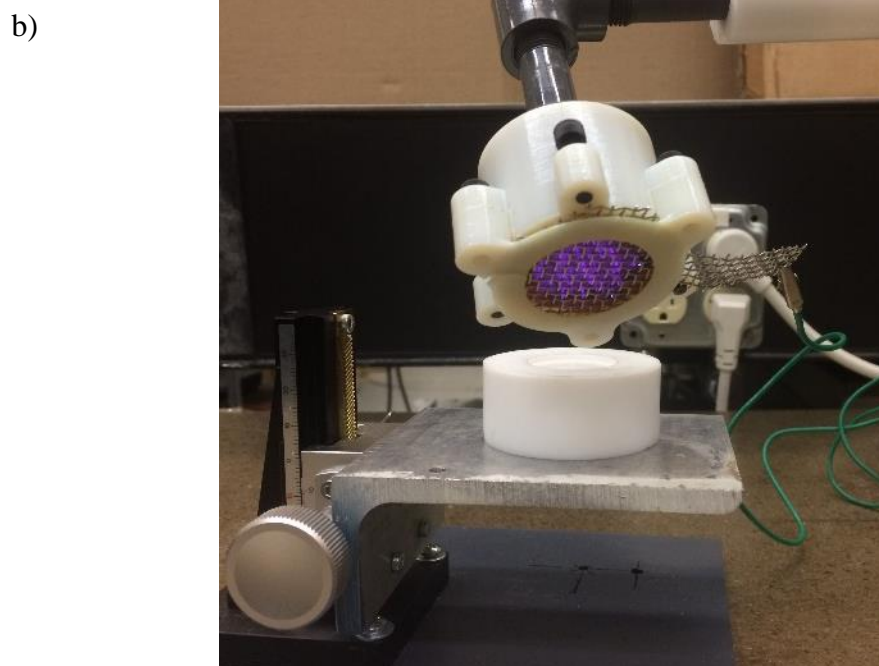
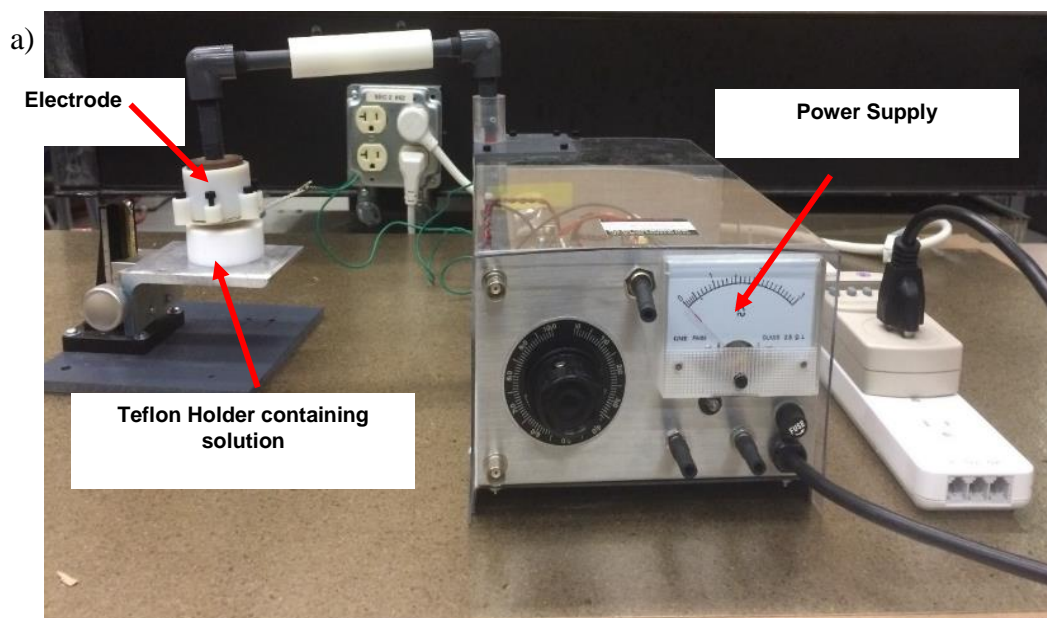


Figure 4: a) Experimental setup for DBD discharge including the power supply, electrode arms, electrode and teflon holder. b) A zoomed in view of the electrode and teflon holder while the system is on is also shown.

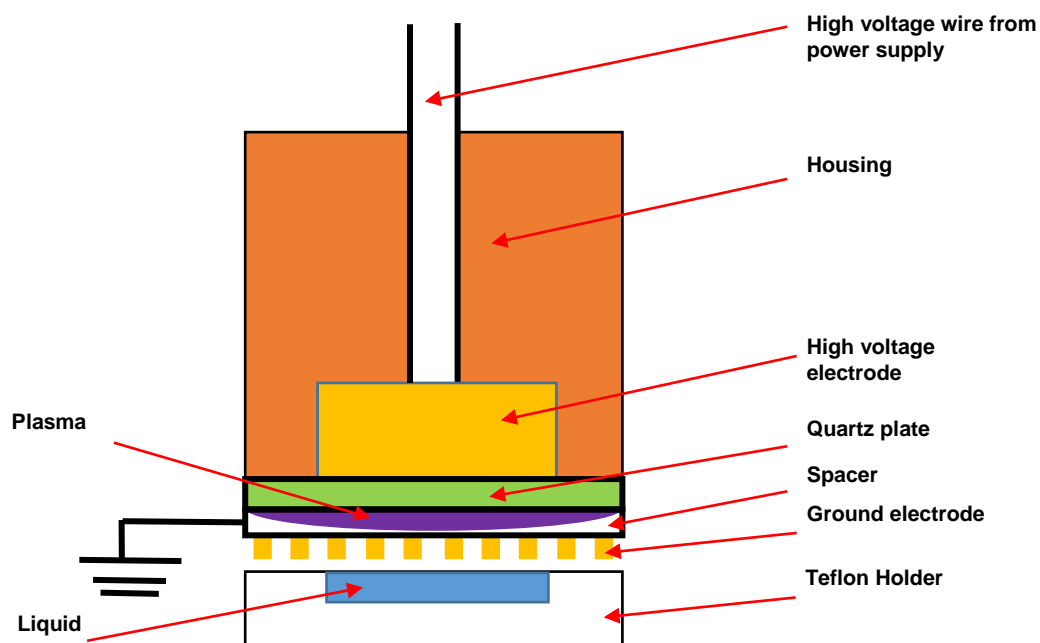


Figure 5: Schematic of the experimental setup (not to scale).

2.3 Proposed Tasks

In order to identify the chemical species responsible for the sporicidal activity of 35% w/w ethanol water solution and to quantify the concentration of the species, several experiments are proposed. These include: a) mass vs time trials, b) pH test, c) UV-Vis-NIR Spectroscopy, d) FTIR Spectroscopy, e) gas chromatography mass spectroscopy (GCMS) and f) colorimetric and enzymatic assay tests for nitrites, nitrates, hydrogen peroxide and other new species formed. Together these tests should help determine the objective to estimate both qualitatively and quantitatively the new species formed after plasma treatment of ethanol-water solutions. Mass vs time trials will help to identify if there are any volatile species formed after plasma activation of ethanol water mixture.

pH test will estimate the decrease in pH of the solutions after plasma treatment. Spectroscopic techniques such as UV-Vis- NIR and FTIR spectroscopy can be used to qualitatively identify the species or functional groups that are formed after plasma treatment. Also, GCMS can be used to separate the new species formed after plasma activation and identify these species. The literature on plasma activation of water shows that concentration of nitrites, nitrates and peroxides are in ppm range [3, 7]. Therefore, in order to quantitatively estimate the concentration of new species formed after plasma activation various detection techniques that are specific for each species such as colorimetric and enzymatic assay tests need to be performed. The colorimetric tests that will be used are Seachem multi test nitrite and nitrate test kit, ferric thiocyanate method for hydrogen peroxide and N,N Diethyl-1,4 Phenylenediamine Sulfate (DPD) test for peracetic acid. The enzymatic assay that will be used is megazyme k-acetrm assay for acetic acid. The details of various enzymatic and colorimetric assays are given in Appendix D.

3 MASS AND ENERGY CALCULATIONS

3.1 Mass vs Time Trials

The 35% w/w ethanol-water mixture before and after plasma treatment was weighed on Sartorius LA230S mass balance with an accuracy of ± 0.1 mg. The normalized evaporated mass for each trial was calculated based on the equation 1, where M_0 is the initial mass of the sample and M is the mass of sample at time t .

$$\text{Normalized Evaporated Mass (NEM)} = \frac{M_0 - M}{M_0} \quad (1)$$

The difference between NEM of treated and untreated samples were taken for all the trials. The average 20 trials are shown in Figure 6. The increase in the difference up to 10 mins indicates the presence of volatile species in the treated mixture which evaporates faster than the untreated mixture within the first 10 minutes.

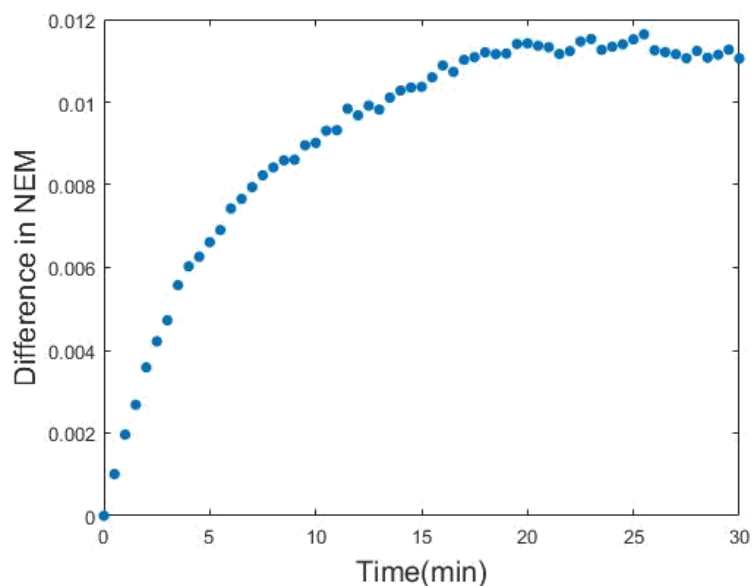


Figure 6: The difference in normalized evaporated mass between treated and untreated ethanol-water mixture. The treated mixture has a higher evaporation rate indicating the formation of volatile species after plasma treatment.

Data was analyzed from the 20 trials for untreated and 25 trials for the treated to identify if there is any statistically significant difference between treated and untreated samples. The t-test for 2 samples were done for the untreated and treated values at different times using SAS 9.8 software for a 95% confidence interval as shown in Appendix B.1. The results are summarized in Table 1. The results show that the difference is statistically significant up to nine minutes and afterwards become negligible. The significant change during the first nine minutes indicates the formation of a volatile species in the treated sample after plasma treatment which was not present in the untreated 35% w/w ethanol-water mixture.

Table 1: Statistical analysis results of mass vs time trials. The results indicate that there is a statistically significant difference in the evaporation from treated sample compared to untreated samples for the first 9 minutes.

Time (min)	Difference in NEM	p-value
0	0	0
2	0.003587	0.00
4	0.006031	0.07
6	0.007427	0.01
8	0.008422	0.03
8.5	0.008593	0.04
9	0.008608	0.05
9.5	0.008956	0.05
10	0.009016	0.07
12	0.009682	0.12
14	0.01028	0.19
16	0.010887	0.25
18	0.011203	0.35
20	0.011421	0.43

3.2 Variation of Input Parameters

The primary input variables of the reactor system are input power, ethanol concentration, activation time and discharge gap. Operating conditions of the system can be changed by changing these variables. To determine the productivity of different experiments and to understand the effect of input variables on the discharge conditions, the output measurements are expressed in different variables. The trends of variation in these parameters with respect to changes in input variables help us to predict reaction changes in the system and deduce appropriate conclusions regarding the observed results.

The mass vs time trials were done to check the dependency on input power, concentration of ethanol, activation time and initial temperature.

3.2.1 Variation with Power

The mass vs time trials for 35% w/w ethanol water solution was done before and after plasma treatment for different powers to check the dependency on power. The average of four trials for different powers is shown in Figure 7. The results indicate that there is an increase in the percentage of volatile species with increasing power. When power is varied, energy density of discharge is changed. Higher the power, higher the input energy into air molecules and so more number of energetic electrons interacting with the air i.e. more number of nitrogen, oxygen and other molecules in plasma can get activated. As a result, the amount of short lived ROS and RONS increase in gas phase due to absorption of more energy. These species interact with the solution kept below and increase the concentration of long lived ROS and RONS in liquid phase. The long-lived ROS and RONS interact with ethanol molecules resulting in the increase in concentration of volatile species.

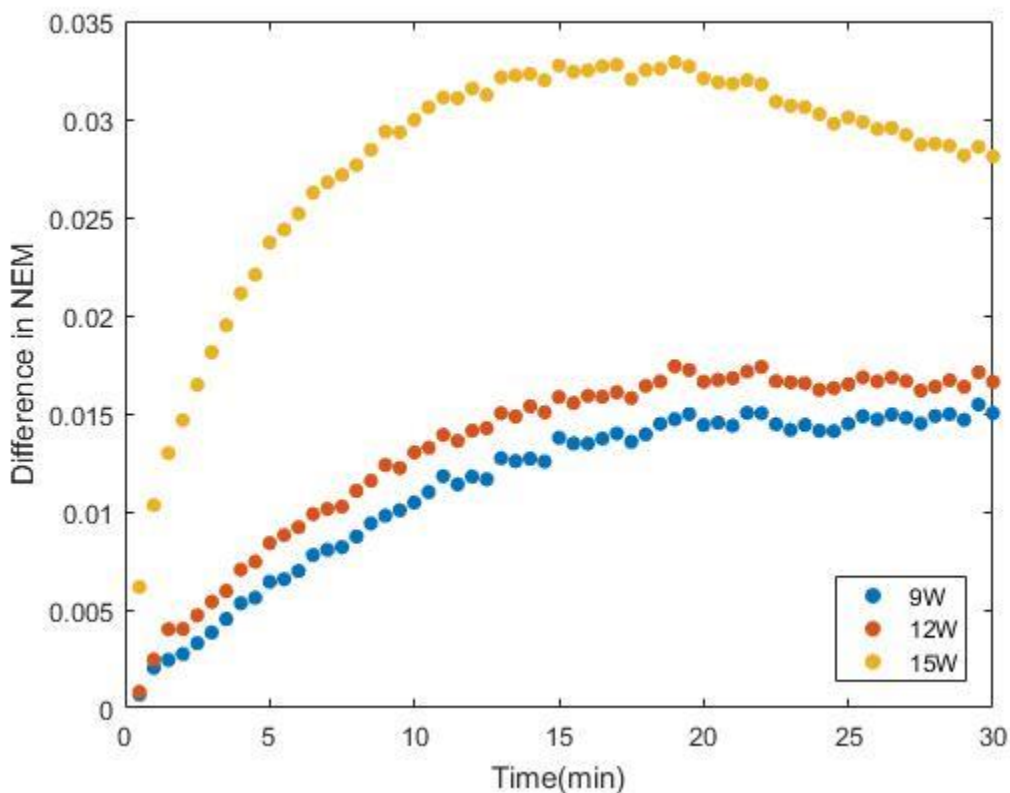


Figure 7: Mass vs time trials for 35 % untreated and treated samples at different powers. The results were repeatable in 4 trials. The percentage of active species in the treated sample was found to increase with increase in power.

3.2.2 Variation with Activation Time

The mass vs time trials for 35% w/w ethanol water solution was done before and after plasma treatment for different activation times. Two trials each were conducted at activation times of 30 secs, 60 secs, 90 secs and 120 sec. The results of the trials are presented in Figure 8. The results indicate that the percentage of the volatile species in liquid phase increase with increase in activation time. Higher the activation time, higher the input energy into air molecules and so more number of energetic electrons

interacting with the air i.e. more number of nitrogen, oxygen and other molecules in plasma can get activated. The subsequent increase in the amount of short-lived and long-lived ROS and RONS results in the increase in the quantity of volatile species coming out of the solution.

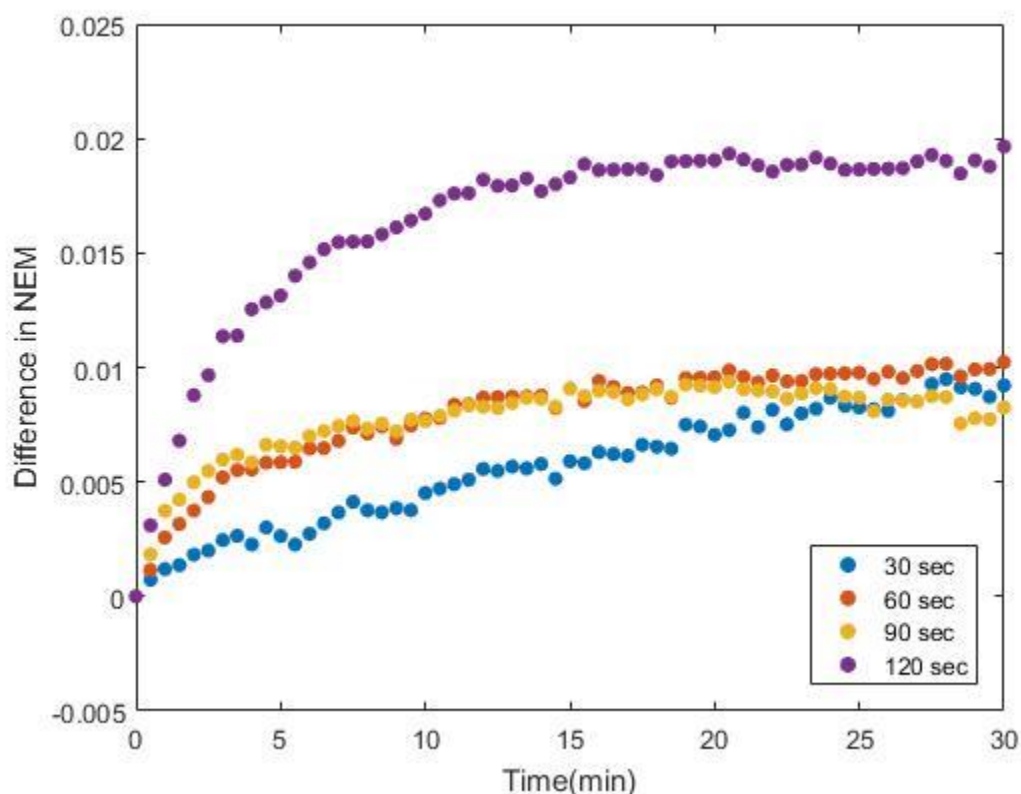


Figure 8: Mass vs time trials for 35 % untreated and treated samples for different activation times. The results were repeatable in 2 trials. There is an observable increase in the percentage of volatile species with increase in activation time.

3.2.3 Variation with Concentration

The mass vs time trials for 35% w/w ethanol water solution was done before and after plasma treatment for concentrations. Two trials each were conducted for 25%,

30%, 35%, 40%, 45% and 50%. The average of the results of the trials are presented in Figure 9. The figure shows no particular trend indicating that there is no significant difference with respect to changes in concentration. There is a decrease in the percentage of new species for higher concentrations (~45-50%) which might be the result of increase in the amount of ethanol evaporating with increase in concentration of interaction ethanol molecules with ambient air. The percent of active species depends more on power, activation times and ambient conditions than with respect to concentration. The variation with concentration has to be investigated further.

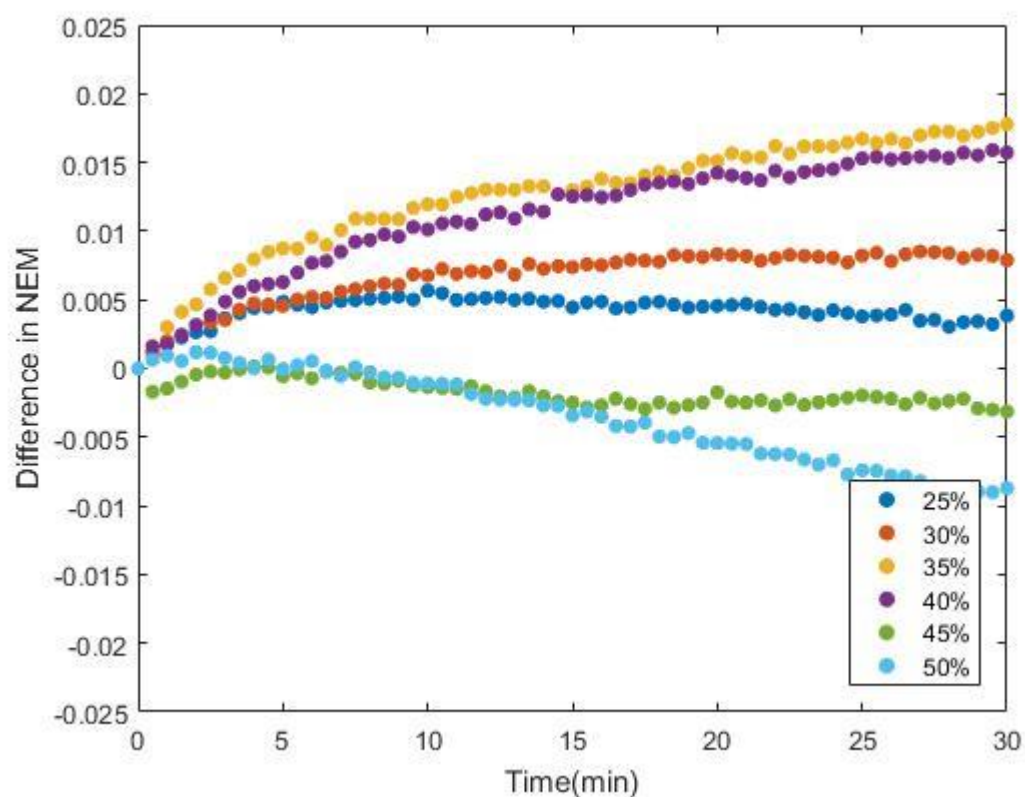


Figure 9: Mass vs time trials for untreated and treated samples for different concentrations. The results were repeatable in 2 trials. No significant dependence on the quantity of volatile species with ethanol concentration was observed.

3.2.4 Variation with Initial Temperature

The mass vs time trials for 35% w/w ethanol water solution was done at different initial temperatures. The trials were repeated for 2 samples. Each sample was first tested at room temperature ($\sim 23^{\circ}\text{C}$). After the tests at room temperature, the sample was cooled to around 17°C . The sample after cooling was heated to around 40°C . The cooling-heating cycle was repeated for 2 samples and the results are shown in Figure 10. The results indicate a strong increase in the percent of new species with increase in temperature. The results are not prominent for the cooled samples ($\sim 17^{\circ}\text{C}$) as the sample return to room temperature quickly ($\sim 23^{\circ}\text{C}$). However, since the temperature during heating ($\sim 40^{\circ}\text{C}$) was large, the sample after plasma treatment was at a higher temperature ($\sim 27^{\circ}\text{C}$) compared to the sample at room temperature. The main reason that temperature increases the rate of reaction is that more of the colliding particles will have the necessary activation energy resulting in more successful collisions. The increase number of collisions with the ethanol molecules results in the increase in the percent of volatile species with increase in temperature. Also, the new species leave faster from the solution at 32°C . The increase in the NEM is probably due to the compounded effect of both these reasons.

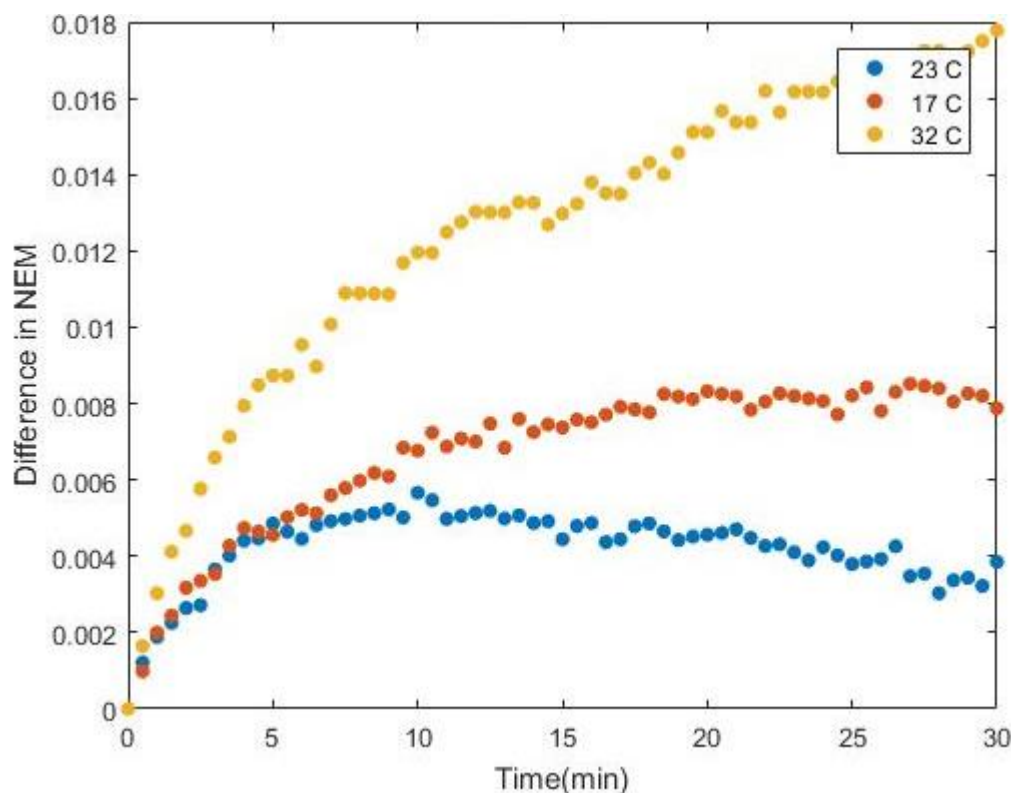


Figure 10: Mass vs time trials for 35 % untreated and treated samples for different temperatures. The results were repeatable for 2 samples. The percentage of volatile species increases with increase in initial temperature.

3.3 pH Test

The measurement of pH for both the treated and untreated samples was performed using OAKTON PC 2700 digital pH meter. The pH meter was calibrated with pH 4, 7 and 10 buffers before use. Also, automatic temperature compensation probe (ATC) was used to compensate for any fluctuations due to change in pH during the test. Literature study has revealed that there is a critical pH of about 4.7 below which the bacteria are effectively inactivated [32]. The decrease in pH in both PAW and PAEW

sare shown in Figure 11. The similarity in pH test (5.4 to 2.8) results indicates that the decrease in pH after plasma activation might not be the reason for the sporicidal activity of PAEW solutions compared to just PAW.

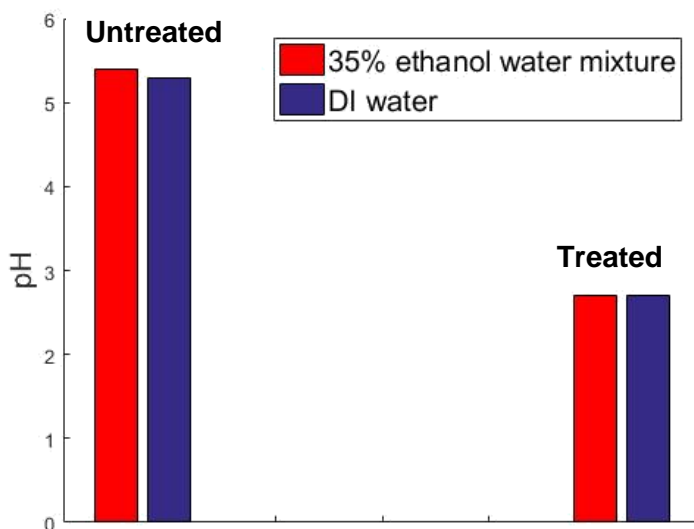


Figure 11: pH test results for both DI water and 35% ethanol water before and after plasma treatments. The results indicate that the decrease in the pH of both water and ethanol-water solutions are similar

3.4 pH Test Calculations

The concentration of H^+ ions and the species can be estimated using the decrease in pH values. The pH of ethanol water mixture was found to decrease from 5.4 to 2.8 after plasma concentration. The approximate concentration of the new species formed after plasma activation are estimated based on the decrease in pH. The detailed calculations for the same are explained in detail in Appendix C. The strong nitric acid

HNO_3 will be fully ionized and we take nitric acid as a reference in our calculations. The combined concentration of species formed after plasma treatment like hydrogen peroxide, nitrites, nitrates and other reactive species are estimated to be between 100-1000 ppm taking into account the uncertainties the plasma production and interaction of reactive species with ethanol water solution after plasma activation.

3.5 Discharge V-I Characteristics

High voltage with a sinusoidal waveform was applied to the planar electrode by using Amazing1 PVM500 plasma resonant and dielectric barrier corona driver power supply. The output power of the power supply was maintained at 13 W using Kill A Watt power meter and the frequency of input voltage was maintained between 22-26 kHz. When the planar electrode was powered, a large number of filamentary discharges with a length of up to approximately 1 mm formed between the dielectric and the perforated electrode. The discharge V-I characteristics of the experimental setup was measured using digital oscilloscope. The output voltage and current for the plasma activated water case and plasma activated ethanol water case was measured using Lecroy Waverunner 204mxi digital oscilloscope as shown in Figure 12. The current signal is shifted in phase from the input voltage and showed a large number of spike-shaped currents, each corresponding to a single micro-discharge. The results indicate that output voltage and current characteristics are similar for both plasma treatments of water and plasma treatment of ethanol water. The steep vertical lines in the current plots

indicates current spikes and streamers. There are a number of additional current spikes present in the ethanol water case. This might be due to the presence of low content of ethanol in air plasma which slightly modifies the reactions in the plasma. Overall the nature of the discharge is similar.

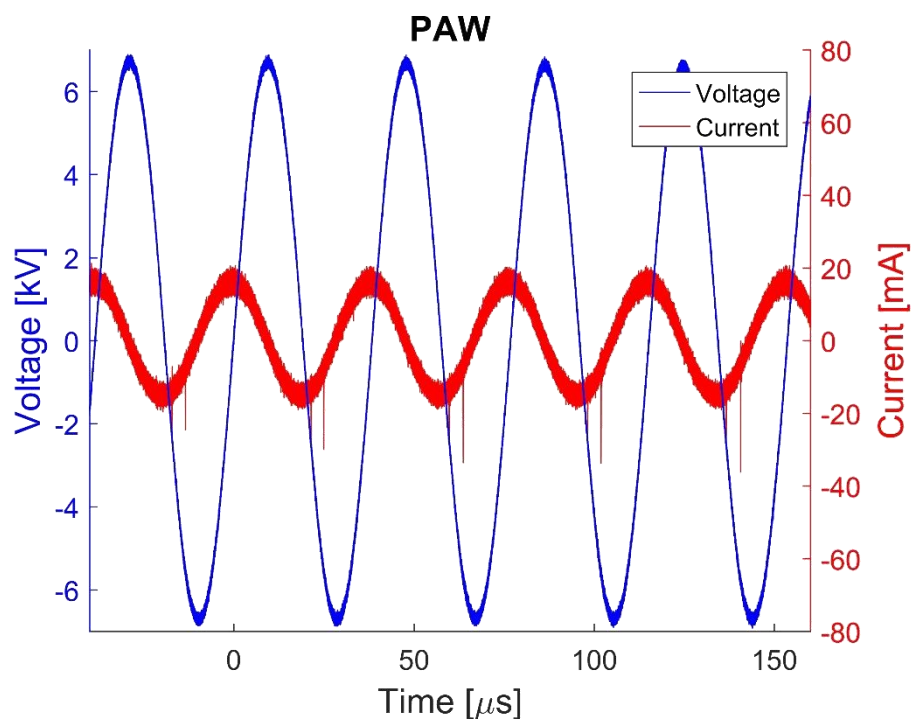


Figure 12: Discharge VI characteristics of the experimental setup in the case of plasma activation of DI water and ethanol water samples. The results are identical indicating the difference in results are due to new species being formed rather than the difference in input conditions.

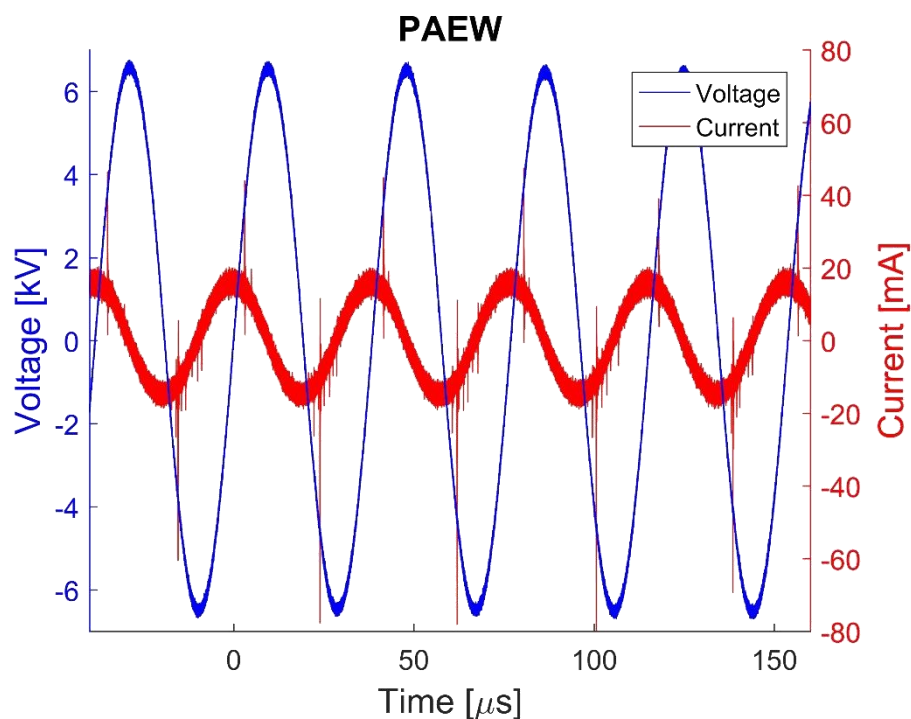


Figure 12: Continued.

The voltage and current is multiplied to get the instantaneous power in both cases as shown in Figure 13. The instantaneous power plot is similar for both cases except for the extra spikes in the case of ethanol water mixture. The power input to the reactor is 13 W as monitored by the wattmeter. The power consumed by the plasma in one cycle is calculated to be 2.11 W as shown in Appendix B.2. The difference in the sporadic activity of plasma treated water and plasma treated ethanol water are probably independent of the discharge V-I characteristics and depend only on the new species formed due to the interactions of air plasma species with ethanol water solution.

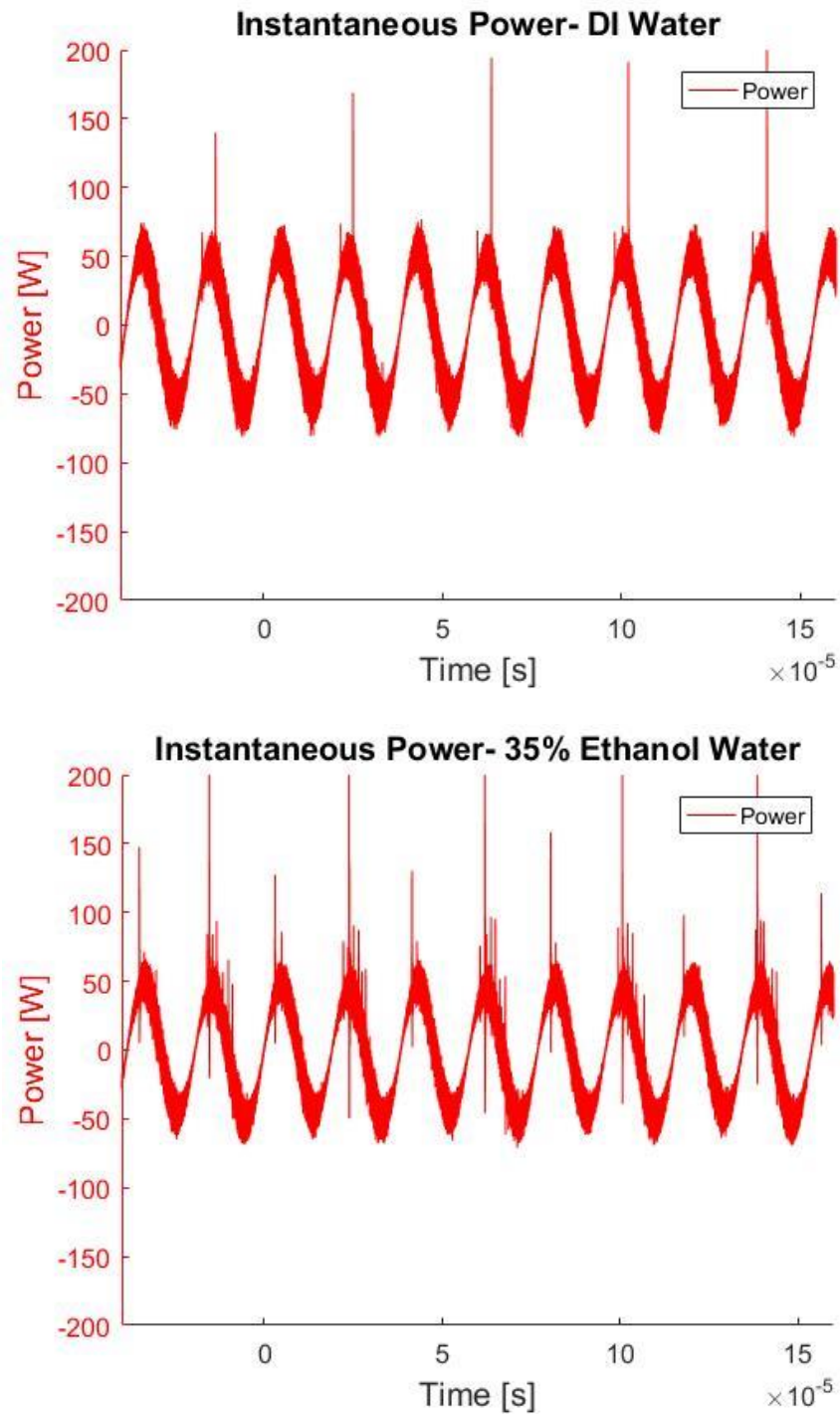


Figure 13: Instantaneous power plots of setup using DI water and ethanol water solution.

3.6 Energy Estimates of Species Generation

The input conditions of the reactor system are kept constant in the experiments conducted. The input power was maintained at 13 W and the frequency was maintained around 23 KHz for the optimum response from the system. The efficiency of conversion of electrical energy to chemical energy can be estimated from the energy input by the power supply and the estimated concentration of species by the pH test. The pH test estimated that the concentration of new species will be in the 1000 ppm range or around 0.1%. The energy conversion efficiency was calculated based on this calculation. The detailed calculations are explained in Appendix C.2. The efficiency of conversion of input electric chemical energy is calculated and found to be around 0.23%. The very low efficiency is due to the configuration of the setup in which there is significant losses due to indirect interaction between the air plasma and the 35% w/w ethanol water solution kept below the reactor setup.

4 QUALITATIVE ANALYSIS

4.1 UV-Vis-NIR Spectroscopy

UV-Vis spectroscopy is transmission or reflectance spectroscopy by using UV and visible light. Shining light in the UV-Vis range on a sample excites bonding electrons. The experiments were carried out with Hitachi U-4100 UV-vis-NIR double beam spectrophotometer at Materials Characterization Facility, TAMU as shown in Figure 14. Preliminary tests done at PEDL shown some variation in absorbance with liquid mixture and more detailed study was done at MCF. The liquid stage was used for the analysis. The spectrometer at MCF had a better resolution compared to the spectrometer at PEDL. Also, the spectrometer at MCF has the additional capacity of taking measurements in the NEAR IR range which can be used to get the characteristic absorption spectrum of various functional groups.



Figure 14: UV-Vis- NIR spectrophotometer at MCF.

4.1.1 UV-Vis-NIR Spectrum for 190- 3300 nm

The absorption spectra of treated sample were taken with reference to untreated sample for wavelengths ranging from 190-3300 nm. Treated minus untreated absorption spectrum for 190-3300 nm taken after 5mins. The absorption spectra of treated sample were taken with reference to untreated sample for wavelengths ranging from 190-3300 nm as shown in Figure 15. In addition to the time dependent behavior around 220-280nm observed at PEDL, a decrease in absorption spectra was observed for wavelengths in the range of 1200-1800 nm and various changes in the 2500-3300 nm finger print range significant spectra are noted. Some of these effects may be due to new species but some may also be due to changes in the concentration of water and ethanol during processing. The location and widths of these peaks is summarized in Appendix C. In general, they occur in two regions around 2739 nm and 3203 nm. Wavenumber and energy corresponding to these are 3651, 3122 cm^{-1} and 0.453, 0.387 eV respectively. When assigning peaks to specific groups in the IR region it is usually the stretching vibrations which are most useful to consider. These relatively high energy bonds accessibly by this technique are only possibly the hydrogen single bonds bending vibrations typically in 3700 – 2500 cm^{-1} range. The most likely candidates are CH (2850-3000 cm^{-1}), OH bound (3000-3400 cm^{-1}), OH free ($\sim 3600 \text{ cm}^{-1}$) and NH (3100-3450 cm^{-1}). The $\sim 3600 \text{ cm}^{-1}$ is most likely the unbounded aqueous OH. The presence of these OH indicates the highly oxidizing nature of the PAEW solution.

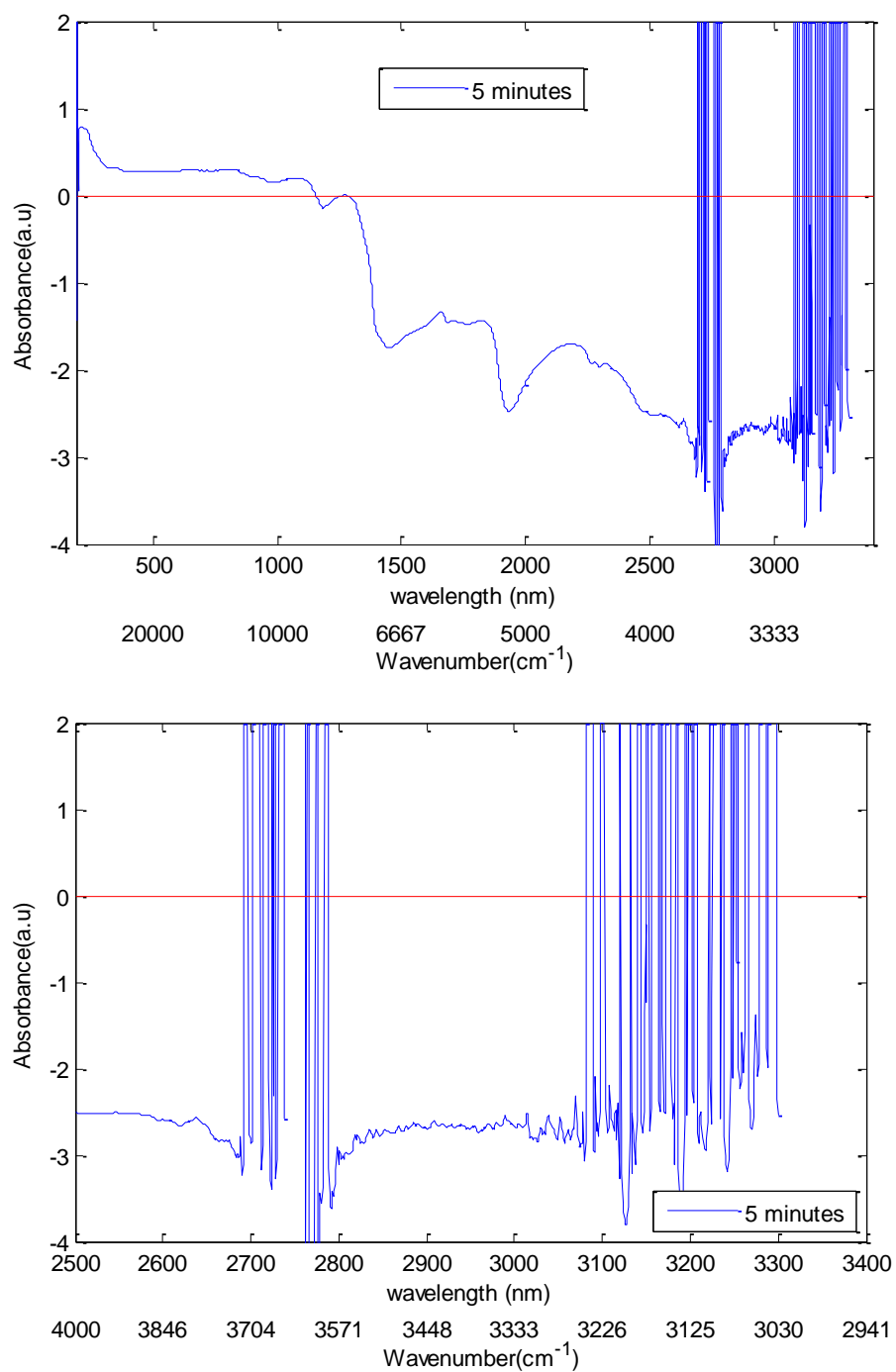


Figure 15: Wavelength dependent absorbance for plasma treated samples of ethanol water mixtures in the 190- 3300 nm range. A zoomed in plot of fingerprint region 2500- 3500 nm is also shown.

4.1.2 UV Spectrum for 200-400 nm

The absorbance of UV light excites bonding electrons in molecules. Absorbance peaks can give information about analyte concentration, reaction progress or sample degradation, charge transfer and band gap. In this experiment, we use UV spectroscopy to identify the presence of new species after plasma treatment. The spectroscopic measurements were done initially for just DI water and then for 35% w/w ethanol water mixture as shown in Figure 16. The spectra of treated samples are significantly different from untreated sample. There is no interference from the spectrum of ethanol and water in this wavelength range. There are possible routes to the formation of acetic and peracetic acid due to the highly oxidative nature of ethanol-water solution after treatment. The new peaks formed after treatment are not definitive yet points to acetic and peracetic acid. The additional shoulder present in the spectra of 35% treated ethanol water mixture is probably due to the absorption peak at 200-220 nm of acetic acid and peracetic acid as given in the literature and database [33, 34]. The 5 peaks around 320 - 380 nm range corresponds to nitrites as given in literature [10]

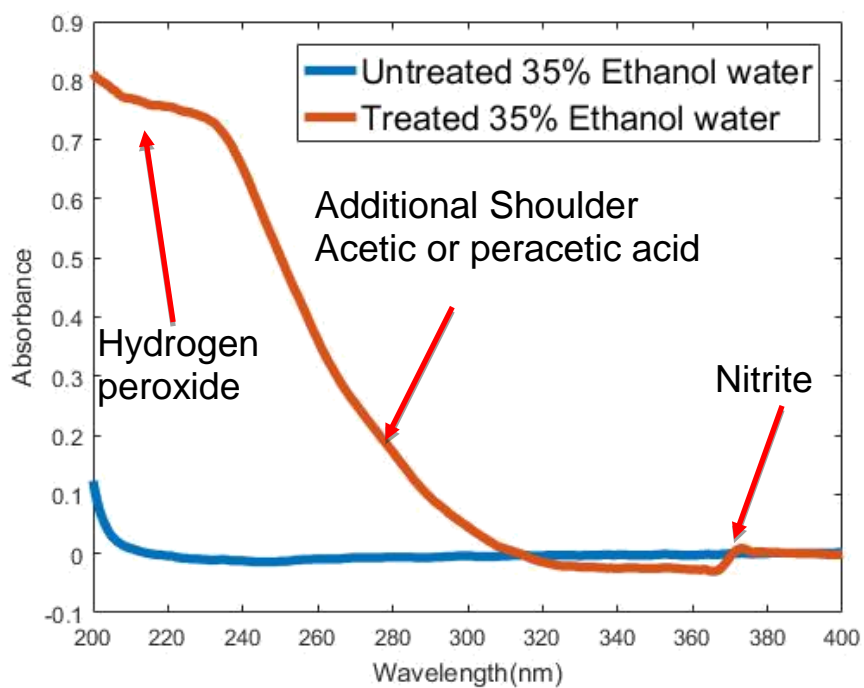
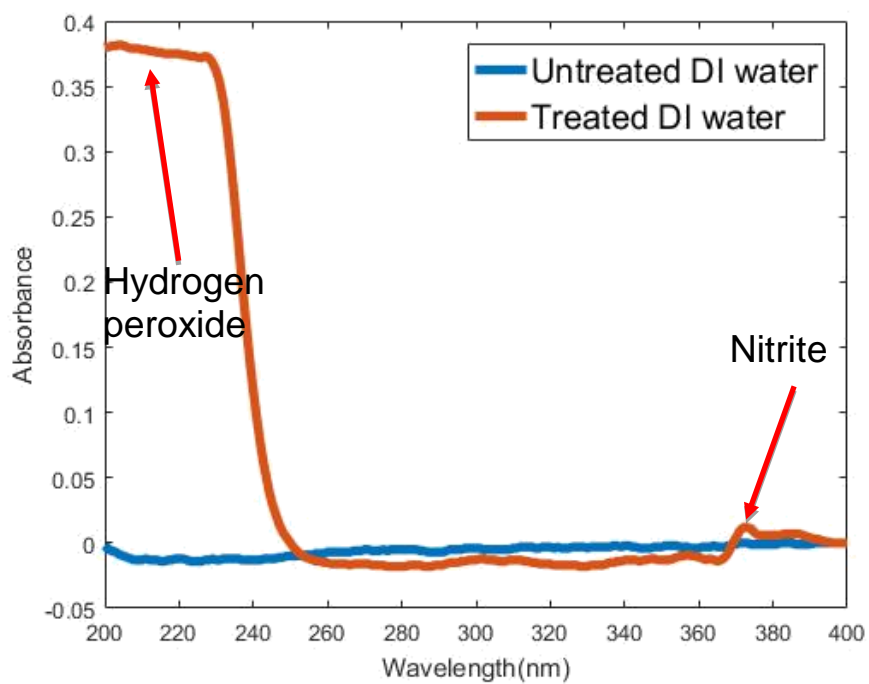


Figure 16: UV Spectrum of DI water and 35% w/w ethanol water solution before and after plasma treatment.

The untreated spectrum was subtracted from the treated spectrum to observe the reaction progress with respect to time. The absorption peaks of the new species were found to decrease with respect to time as shown in Figure 17. The 35% ethanol water mixture after plasma treatment has very high oxidizing characteristics. The decrease in the concentration of nitrites and acetic acid probably indicates that these species are being oxidized.

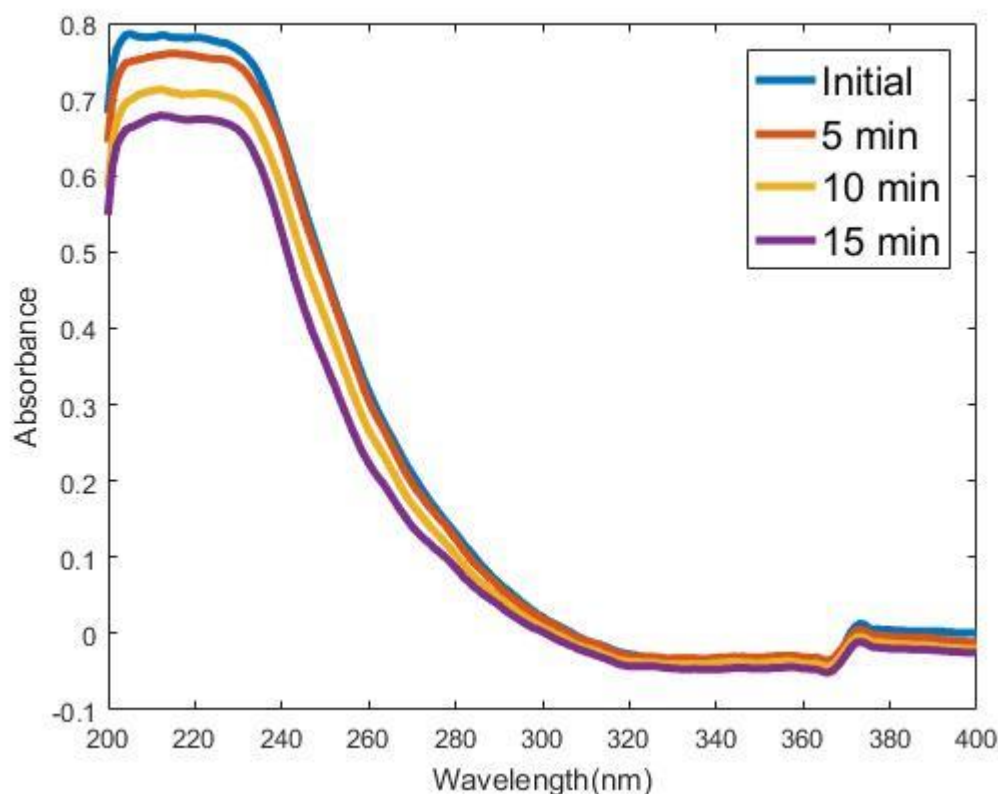


Figure 17: Time dependent UV spectrum of 35% ethanol water mixture after plasma treatment. The decrease in the absorbance values after plasma treatment indicates the decrease in concentration of new species with respect to time.

The mass vs time trials confirmed the formation of volatile species after plasma treatment. The UV spectrum of the vapors coming out of both the untreated and treated

35% ethanol water mixtures are shown in Figure 18. The untreated vapor phase spectrum consists of just the absorption peaks of ethanol. However, the treated mixture has an additional shoulder in the 200 nm to 240 nm indicating the presence of new volatile species after plasma treatment. Literature study indicates these peaks might possibly be due to peracetic acid which is formed by the oxidation of acetic acid.

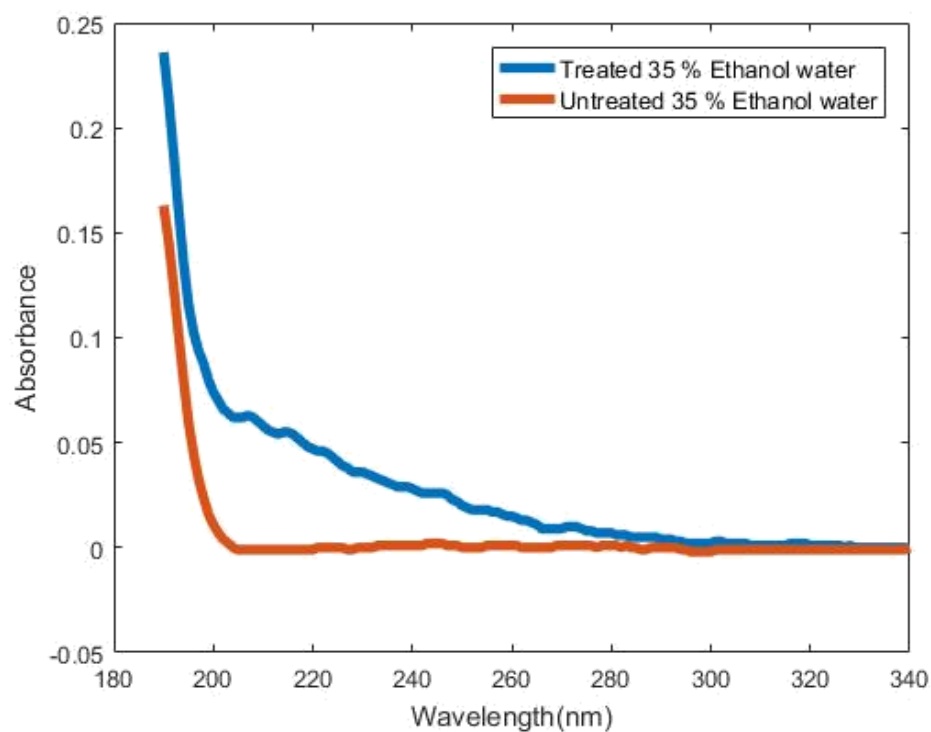


Figure 18: UV spectrum of vapors coming out of 35% ethanol water mixture after plasma treatment. The presence of an additional shoulder in the 200 nm to 240 nm in the treated spectrum indicates that these absorbance peaks are due to the volatile species coming out of the mixture formed due to plasma treatment.

4.2 ATR-FTIR Spectroscopy

Infrared (IR) spectroscopy looks at the vibrational motion of bonds in molecules. By identifying the types of bonds present in a certain compound, it is possible to gain insight into the compound structure. Infrared spectrometer gives us an understanding of the structure of the compound by analyzing its vibrational motion. The wavelength and energies of the vibrational motion will be characteristic of a particular functional group. The experiments were carried out with Thermo Nicolet 380 FTIR spectrometer at Materials Characterization Facility as shown in Figure 19. Infrared spectroscopy is a vibrational spectroscopy technique. Mid and far IR light is shined on a sample. The diamond tipped ATR stage was used for FTIR measurements. Fourier transform infrared spectroscopy (FTIR) identifies chemical bonds in a molecule by producing an infrared absorption spectrum. Covalent bonds absorb the energy of the light and vibrate at a frequency characteristic of the bond energy. FTIR peaks are characteristic in energy and shape for specific chemical functional groups. FTIR spectra can be used to elucidate chemical structure, pinpoint formation of reaction product and identify chemical functionalization of material. Attenuated total reflectance spectroscopy is reflective method during which total internal reflection of light in crystal results in an evanescent wave. Light is amplified by crystal with high refractive index such as Diamond, ZnSe, Ge, Si. The penetration depth in microns dependent on crystal refractive index.



Figure 19: The Diamond tipped ATR stage and Thermo Nicolet 380 FTIR spectrometer.

The absorption spectra of treated and untreated 35% ethanol water solution were taken separately for wavenumbers ranging from $500\text{-}4000\text{ cm}^{-1}$ as shown in Figure 20. However, there is no significant difference between the treated and untreated spectra other than the results caused by ethanol evaporation. The results of ATR FTIR spectroscopy did not indicate any strong absorption peak for acetic acid. However, it might be possible that the concentration of acetic acid might be below the detection limit of the instrument. Also, the new peaks are probably masked by the strong absorption peak of water at 1600 cm^{-1}

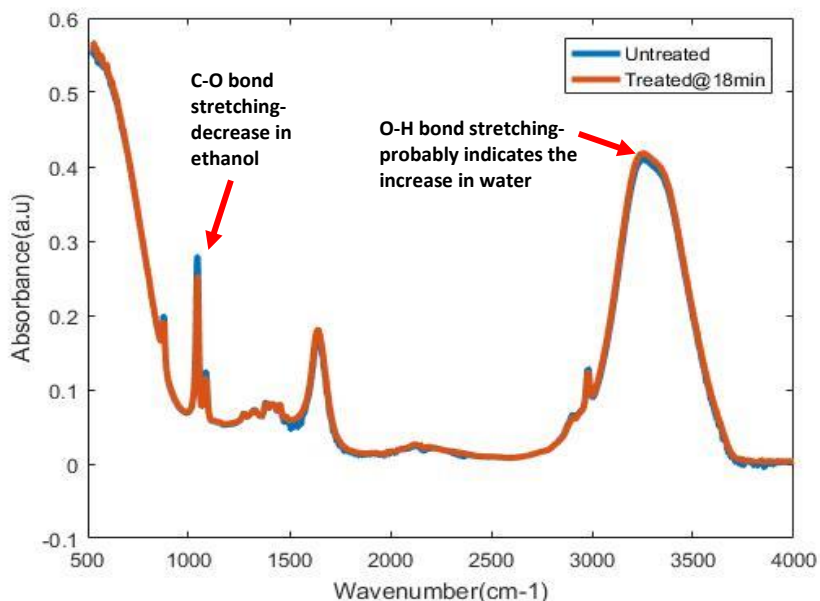


Figure 20: FTIR absorption spectra of the untreated and plasma treated samples of 35% w/w ethanol-water solution. There appears to be no significant change other than the small relative concentration increase of water and decrease in ethanol due to evaporation.

4.3 GCMS

The GCMS was performed on Ultra GC/DSQ (ThermoElectron, Waltham, MA) using electron impact ionization (EI) at the Chemistry Mass Spectrometry Facility as shown in Figure 21. Rxi-5ms was used as a gas chromatographic column with dimensions of 60 m length, 0.25 mm ID and 0.25 μm film thickness (Restek; Bellefonte, PA). Helium was used as a carrier gas at constant flow of 1.5 ml/min. The injection volume was 1 μL . The splitless injection technique was used as the concentration of new species is low as is evident from the previous spectroscopic analysis. The gas chromatogram starts showing output before the column gets heated indicating that there

is a co-elution of all the species indicating that the mass spectrum is the superposition of spectra of different species. The gas chromatogram data is taken directly from the Xcalibur Software. The raw data from the mass spectra is acquired and plotted using MATLAB.



Figure 21: GCMS setup at Chemistry Mass Spectrometry Facility.

The GCMS was done of DI water within 1-2 minutes of plasma treatment. The GCMS log plots for various elution times are shown in Figure 22. The results indicate the formation of new species in the m/z 45-49 range. The m/z 47 is most probably nitrous acid(HNO_2) formed due to the interaction of NO radical with water [35]. The peaks between m/z 80 - m/z 90 were not identified.

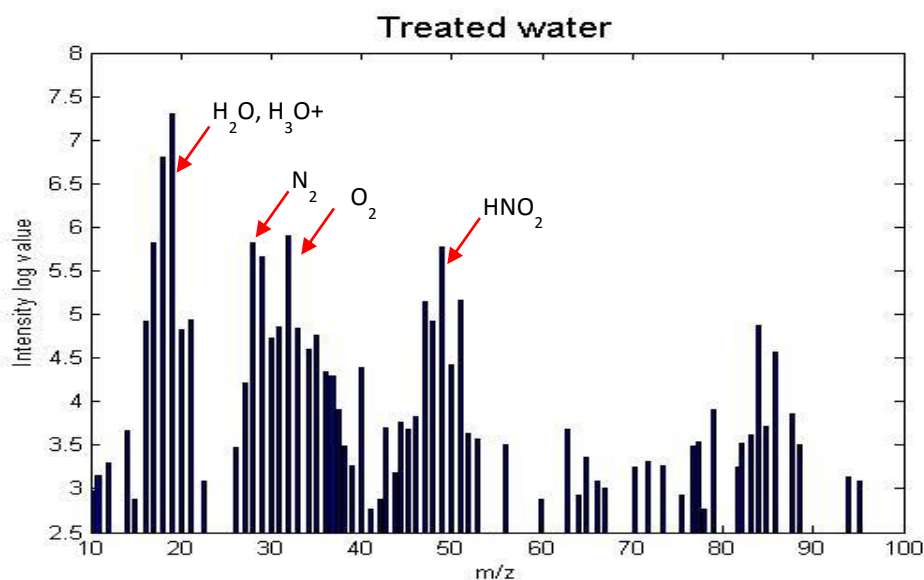


Figure 22: GCMS spectra of plasma treated DI water solution. The identified species are labelled as shown.

The GCMS tests were done for 35 % ethanol water solution before and after plasma treatment and the results are shown in Figure 23. Because of superposition and lack of calibration we can infer only qualitative results from the results. The peaks below intensity log value of 4 are most probably noise. The most notable difference is the increase in intensities of the peaks at m/z 49, m/z 60 and m/z 76. The m/z peak at 60 is possibly acetic acid. The peaks for nitrites and nitrates will be at m/z 46 and m/z 30 as given in literature [35]. These peaks are not distinguishable as the concentration is in ppm level (from the colorimetric tests at lab) and there are strong peaks from ethanol in that region. The mass spectra of ethanol, water and acetic acid are compared to PAEW as shown in Figure 24 [36]. Further study is required to explain the peaks at m/z at 49,

m/z at 76 and various other peaks that might be present in low intensities. The possibility that peaks might also be the background or due to the compounds present in column should also be considered.

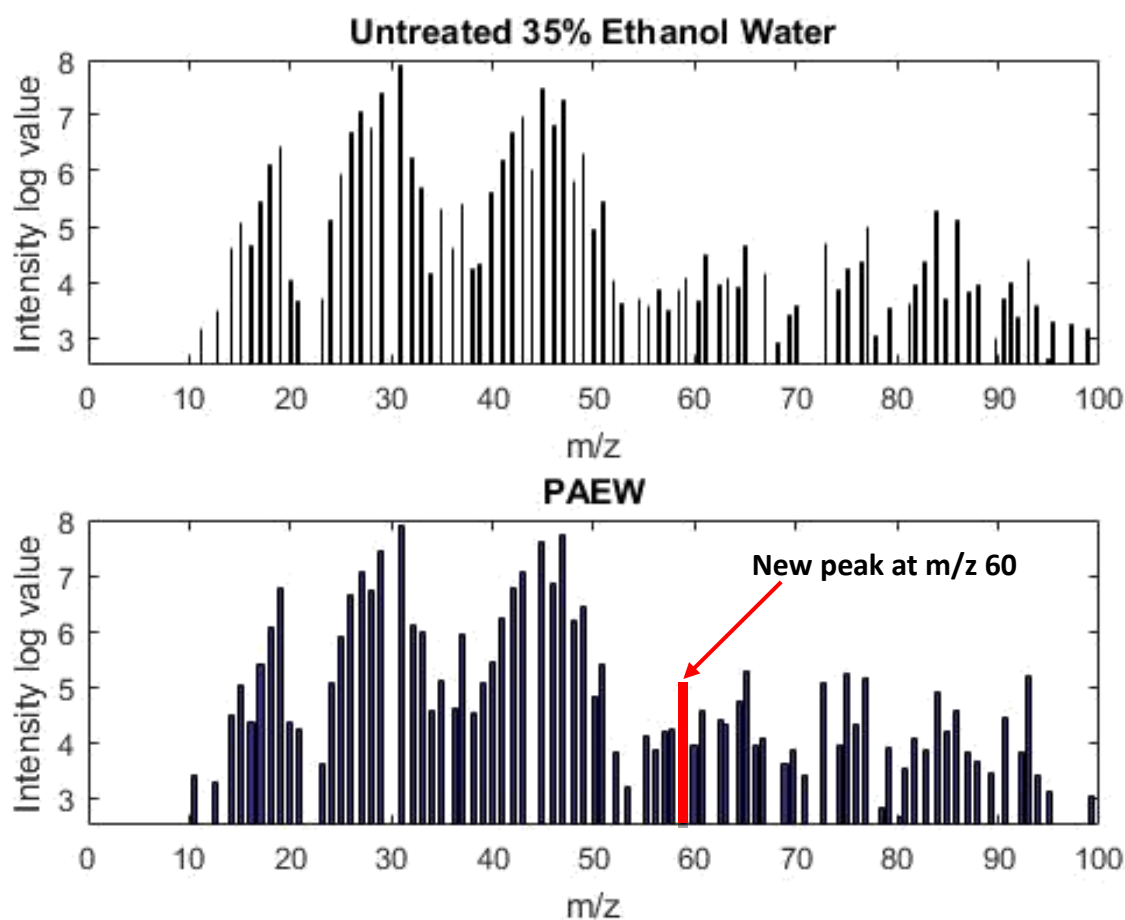


Figure 23: Mass spectra at same elution time ($t = 3.85$ sec) for ethanol water mixture before and after plasma treatment. The post discharge spectra possibly indicate the presence of nitrates, nitrites and acetic acid.

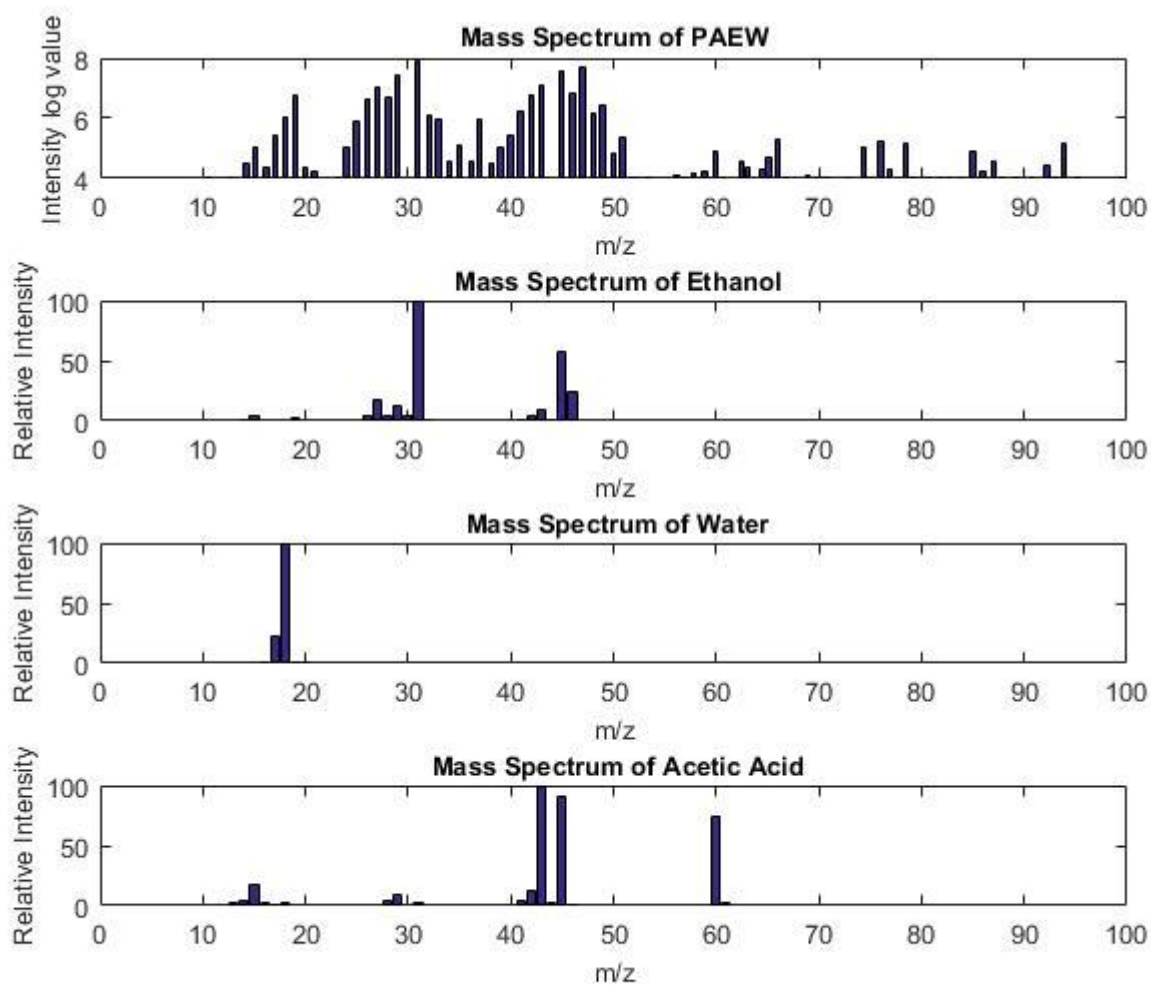


Figure 24: Comparison of mass spectra of PAEW with individual spectra of ethanol, water and acetic acid.

The GCMS tests were done for 35 % ethanol water solution for three different activation times i.e. untreated, treated for 1 minute, treated for 5 minutes and treated for 10 minutes and the results are shown in Figure 25. The results probably indicate the increase in the concentration of acetic acid with increase in activation time.

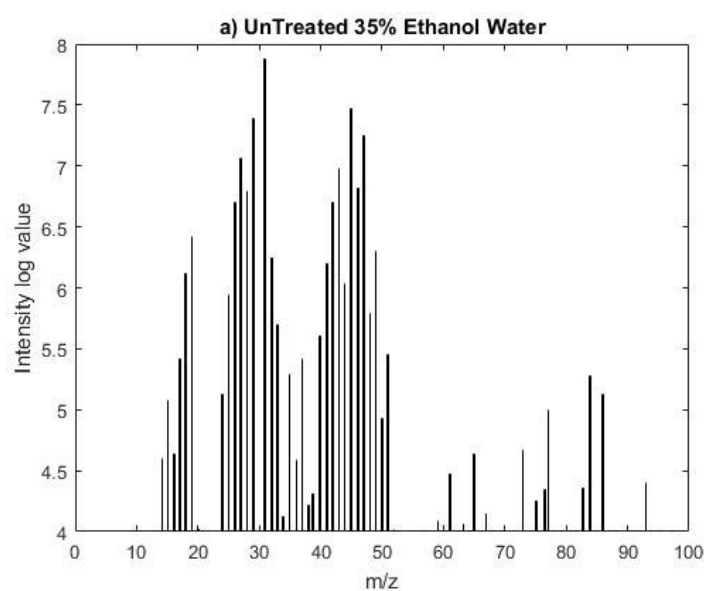


Figure 25: Mass spectra at same elution time ($t = 3.85$ sec) for ethanol water mixture before and after treatment for different activation times. The post discharge spectra possibly indicate the increase in concentration of acetic acid with increase in activation times.

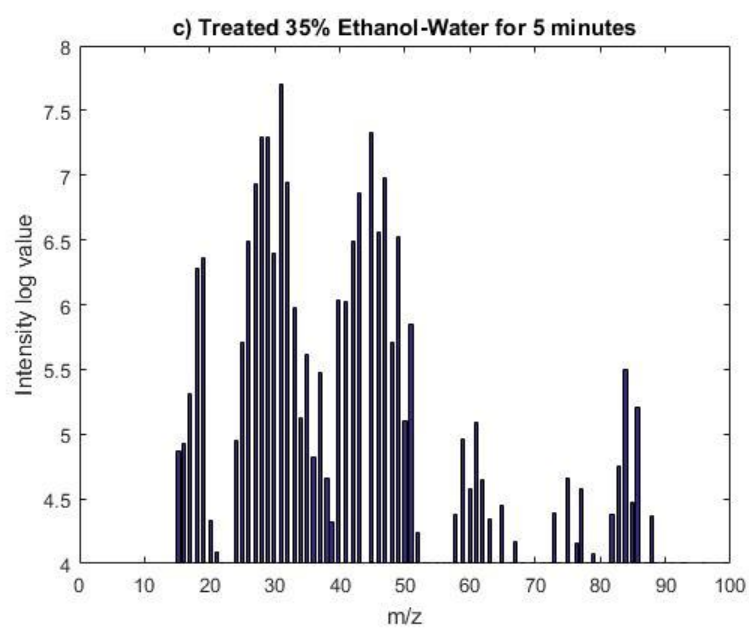
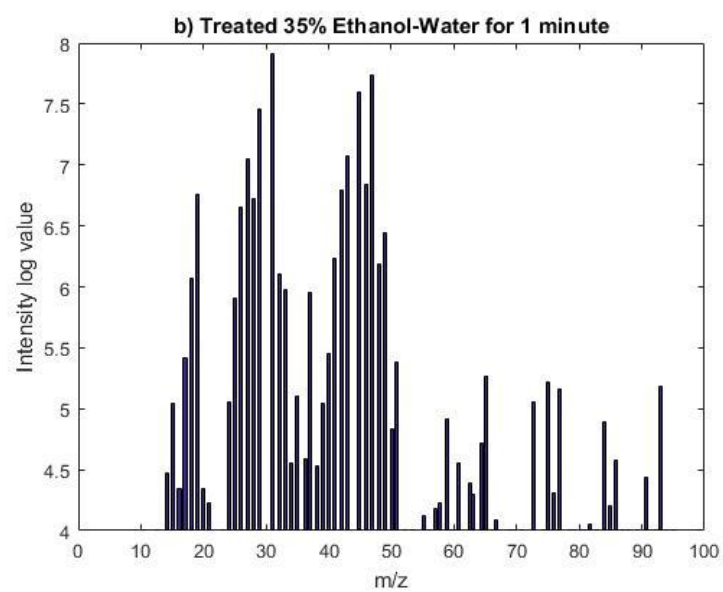


Figure 25: Continued.

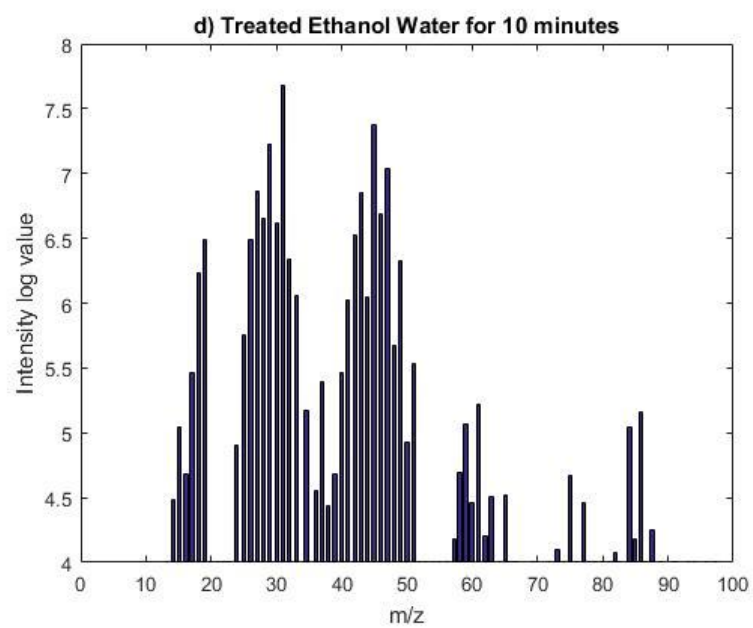


Figure 25: Continued.

5 QUANTITATIVE ANALYSIS

The UV-Vis-NIR spectroscopy, GCMS and the extensive literature available for plasma activated water gave an idea about the presence of nitrites, nitrates and hydrogen peroxide in the ppm range after plasma activation. The presence of new species like acetic acid and peracetic acid was also indicated in the qualitative tests. However, the exact concentration these new species were not determined during these tests.

Colorimetric analysis is a method of determining the concentration of a chemical element or chemical compound in a solution with the aid of a color reagent. It is applicable to both organic compounds and inorganic compounds and may be used with or without an enzymatic stage. The aqueous phase chemistry was analyzed via specific assays for nitrate, nitrite, hydrogen peroxide, acetic acid and peracetic acid. The interferences from various species while testing for a particular species was also taken into account during these tests.

5.1 Detection of Hydrogen Peroxide

Hydrogen peroxide is a strong oxidizing agent. Hydrogen peroxide was detected in the UV-Vis Spectroscopy trials mentioned in section 4.1.2. In order to determine the concentration of hydrogen peroxide in 35% ethanol water solution after treatment, hydrogen peroxide test kit by Chemetric Inc. (VACUettes visual high range kit) was used. The test kit uses ferric thiocyanate method to detect hydrogen peroxide. The ferric

thiocyanate method consists of ammonium thiocyanate and ferrous iron in acid solution. In an acidic solution, hydrogen peroxide oxidizes ferrous iron. The resulting ferric ion reacts with ammonium thiocyanate to form ferric thiocyanate, a red-orange colored complex, in direct proportion to the hydrogen peroxide [21]. Results are expressed as ppm (mg/L) H_2O_2 . The possible interfering species are peracetic acid. But the presence of peaks in the UV spectrum confirms the presence of hydrogen peroxide and the test gives a general idea regarding the concentration range of hydrogen peroxide.

The PAEW was allowed to mix with reagents present in the ampoule after plasma treatment as shown in Figure 26. The ampoule was then compared with the comparator to identify the concentration range of hydrogen peroxide after treatment. The untreated liquid didn't produce any color change indicating the absence of hydrogen peroxide. The 35% ethanol water mixture after treatment on reaction with the contents of the ampoule turns into a light red color confirming the presence of hydrogen peroxide. The tests were repeated with 35% ethanol water mixture for different post discharge times. However, no significant color change was observed indicating that there is not much difference in the concentration of hydrogen peroxide with times. The concentration of hydrogen peroxide in the 0.6 ml sample after plasma treatment was found to be around 120-240 ppm and it is found to remain stable in this range for up to 20 minutes.

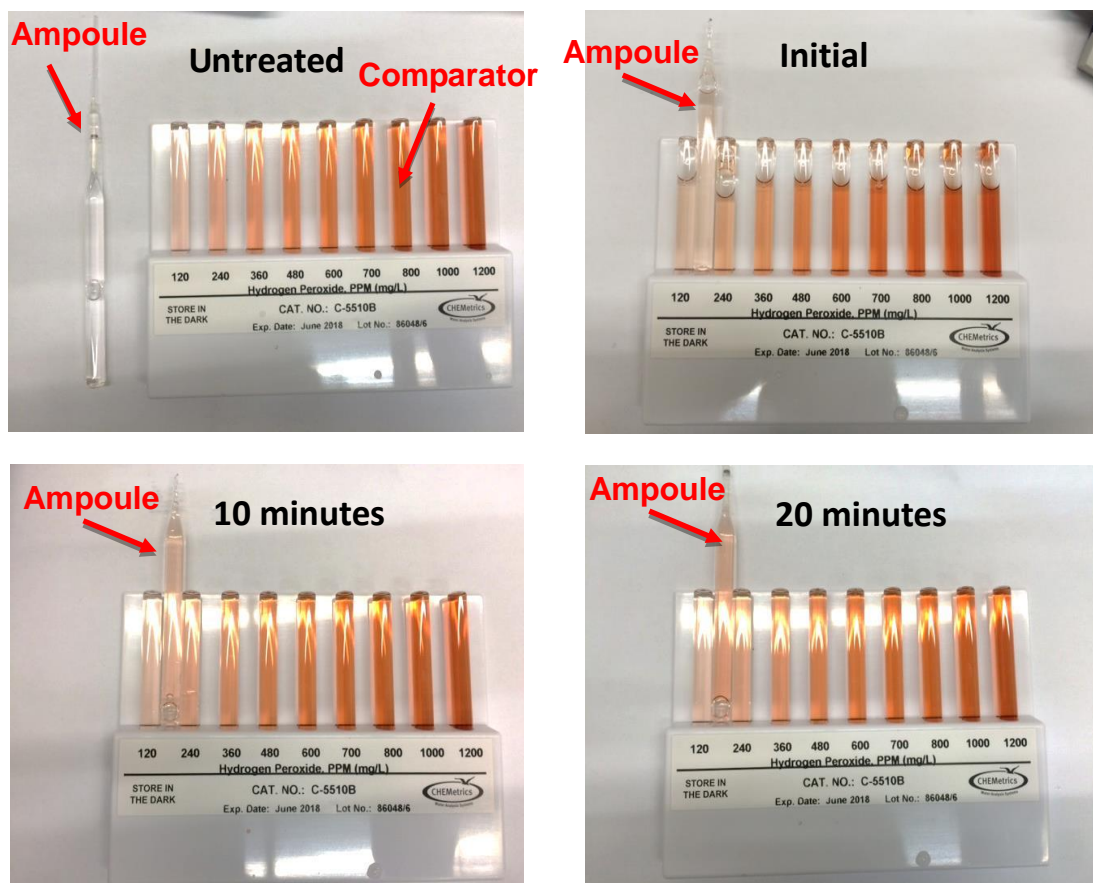


Figure 26: Hydrogen peroxide detection for PAEW using Chemtrics VACUettes visual high range kits. The times mentioned are wait times from treatment to test. The hydrogen peroxide concentration was found to be in the 120-240 ppm range and it was found to remain stable with time.

The hydrogen peroxide was also detected with Lamotte Peracetic Acid Test kit [37]. The test kit can also be used to test both peracetic acid and hydrogen peroxide using different titration techniques. The PAW and PAEW was mixed with hydrogen peroxide titrant. Both the solutions turned a pale yellow color indicating the presence of hydrogen peroxide as shown in Figure 27. The concentration of hydrogen peroxide in

both plasma treated water and plasma treated ethanol water after 1-minute treatment is in the 200 ppm range.

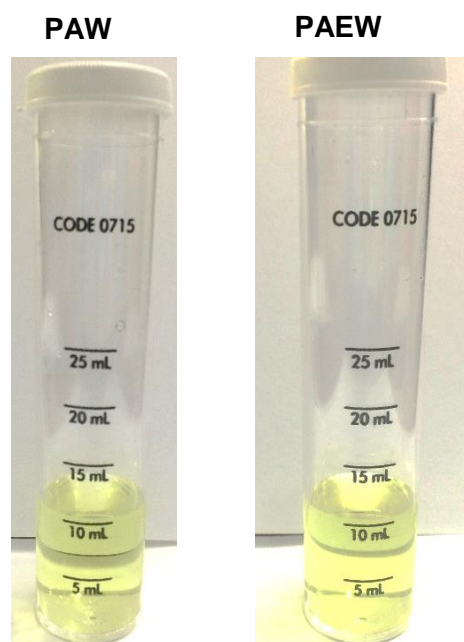


Figure 27: Hydrogen peroxide detection using Lamotte test kit. The test kit produced similar test results as the Chemtrics test kit. Also, the hydrogen peroxide concentration in both PAW and PAEW solution are in the 200 ppm range.

5.2 Detection of Nitrites and Nitrates

The presence of nitrites and nitrates in plasma treated water by many is well documented by many research groups [3]. The presence of nitrites were observed in the UV-Vis Spectroscopy trials mentioned in section 4.1.2. The decrease in pH of plasma activated water was mainly due to the formation of nitrates after plasma treatment [10]. The PAW mixture was diluted with 0.5 ml of distilled water and the mixed with reagents

for nitrite and nitrate using Seachem multitest nitrite and nitrate kit as shown in Figure 28. The test was then repeated for PAEW. The presence of nitrites and nitrates were observed. Nitrite concentration was observed to be 50-100 ppm and nitrate concentration was observed to be 100 – 200 ppm in PAW and PAEW. Additionally, PAEW was tested for the presence of nitrite and nitrate for different post discharge times and the results are shown in Figure 29. The results indicate that initially nitrite concentration is above 25 ppm and it disappears within the first 20 minutes. The nitrate concentration remains almost the same with time. The possible explanation is the oxidation of nitrite to nitrate by various oxidizing species formed after plasma treatment.

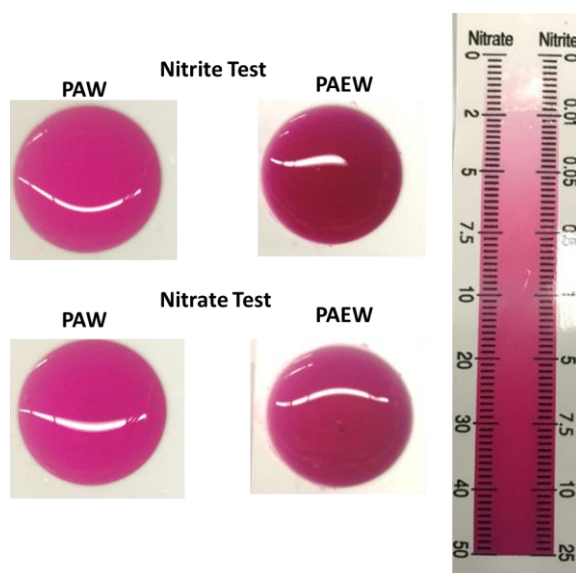


Figure 28: Nitrite and nitrate detection using Seachem multitest nitrite and nitrate test kit

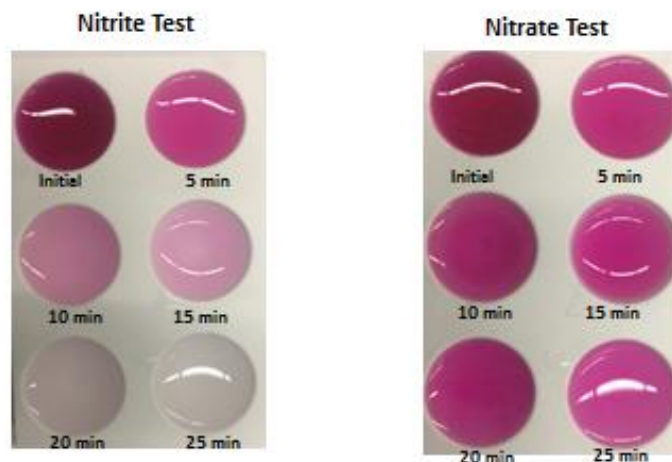


Figure 29: Nitrite and nitrate detection using Seachem multitest nitrite and nitrate test kit for different post discharge times for PAEW. The times mentioned are wait times from treatment to test. The nitrite concentration is found to decrease within the first 20 minutes.

5.3 Detection of Acetic Acid

The UV Vis trials and GCMS trials indicated the formation of acetic acid after plasma treatment of 35% ethanol water mixture. To confirm the presence of acetic acid and estimate the concentration of acetic acid after plasma treatment Megazyme K-ACETRM enzymatic assay was used. This assay is specific for acetic acid. It is a spectrophotometric assays by which we can estimate the concentration of an assay by its absorbance at a particular wavelength in the UV region and comparing it to the absorbance of a known concentration of solute at that particular wavelength. UV light is often used, since the common coenzymes NADH and NADPH absorb UV light in their reduced forms, but do not in their oxidized forms. The absorption measurements

were done by the UV-Vis-NIR spectrophotometer at the Materials Characterization Facility.

The principle of the assay is shown in detail in Appendix E. The decrease in the absorbance of NADH at 340nm was measured by the UV-Vis-NIR spectrophotometer at the Materials Characterization Facility. The concentration of acetic acid can be estimated

using the below equation
$$2 \frac{V * MW}{\epsilon * d * v}$$

$$\text{Acetic Acid(g/L)} = \frac{V * MW}{\epsilon * d * v} * \Delta \text{Abs} * F \quad (2)$$

where

V = final volume [mL]

MW = molecular weight of acetic acid [g/mol]

ϵ = extinction coefficient of NADH at 340 nm

d = light path [cm]

v = sample volume [mL]

F = Dilution factor

The absorbance values are significant when the $\Delta \text{Abs} > 0.1$. The results of the trials for the 0.6ml 35% ethanol water treatment for different dilutions are shown in table 2. It has been found that dilution by a factor more than 10 results in $\Delta \text{Abs} < 0.1$ which is ignored. The results indicate that concentration of acetic acid is in the 90-300 ppm range. Each trial is a separate trial from plasma activation to absorbance measurement. Sources of variability are 1) manual error with titration 2) variability in acetic acid formed after plasma treatment 3) time dependent behavior of acetic acid.

Table 2: Spectrophotometric results of PAEW

Trial No	Dilution	Δ Abs	Acetic Acid(mg/L)
1	1	0.654	165
2	1	0.359	91
3	1	0.83	210
4	1	1.049	265
5	5	0.212	268
6	5	0.158	200
7	10	0.107	271
8	20	0.081	410
9	50	0.042	532

Time dependent absorbance trials were performed to observe if the decrease in absorbance of the analyte is similar to the theoretical absorption curve. The results of three trials are shown in Figure 30. The decrease in the NADH absorbance of the PAEW is similar to the theoretical absorption curve as given by Megazyme confirming the presence of acetic acid. The uncertainties in the experimental absorption curve are due to differences in the initial conditions, temperature, humidity and manual error during plasma treatment.

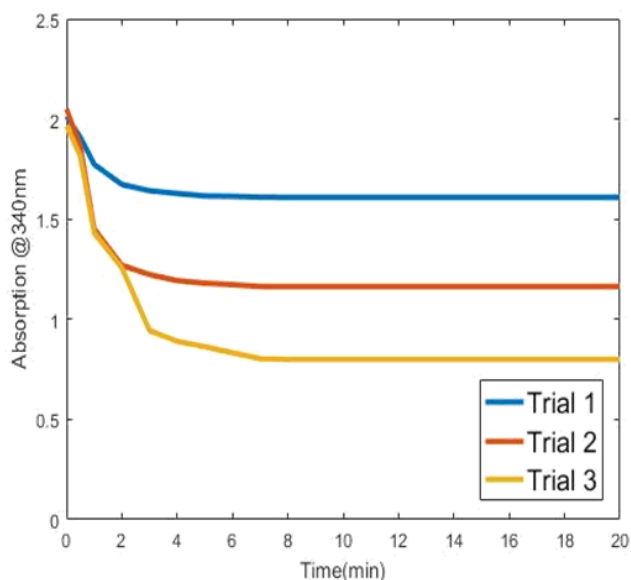


Figure 30: Experimental absorption curve of the decrease in the absorbance of NADH with time. The three trials are done at standard operating conditions for plasma generation and dilution factor, $F=1$.

5.4 Detection of Peracetic Acid

The presence of acetic acid is confirmed by the enzymatic assay test. The UV trials in the vapor phase and the mass vs time trials indicated the formation of peracetic acid which has a boiling point of 25°C . The shoulder in the liquid phase also probably indicates peracetic acid. It is formed by the reaction of acetic acid with hydrogen peroxide in acidic medium[38]. The PAEW solution contains acetic acid, hydrogen peroxide and nitrates which are suitable conditions for the formation of peracetic acid. The presence of peracetic acid was confirmed using the Lamotte peracetic acid test kit [37, 39]. The results of the trials for both PAW and PAEW are shown in Figure 31. The solution will turn a cloudy brown color during titration if peracetic acid is present.

Peracetic acid was detected in PAEW with concentration in the range of 200 ppm. The test didn't give any results for PAW indicating that there might not be interferences from nitrites, nitrates or hydrogen peroxide. The possible interference is from acetic acid and it is checked by repeating the test with vinegar. The results are similar to PAW indicating that there is no interference from acetic acid for the formation of cloudy brown color during PAEW test.

The peracetic acid is a strong sporicidal agent [40] and the boiling point of peracetic acid is 25°C. The presence of peracetic acid can explain the vapor phase UV trials and the mass vs time trials. The plasma treatment of ethanol water solution raises the temperature of solution by 2-3°C. The mass loss during the mass vs time trials are probably due to the loss of ethanol and peracetic acid during the plasma treatment.

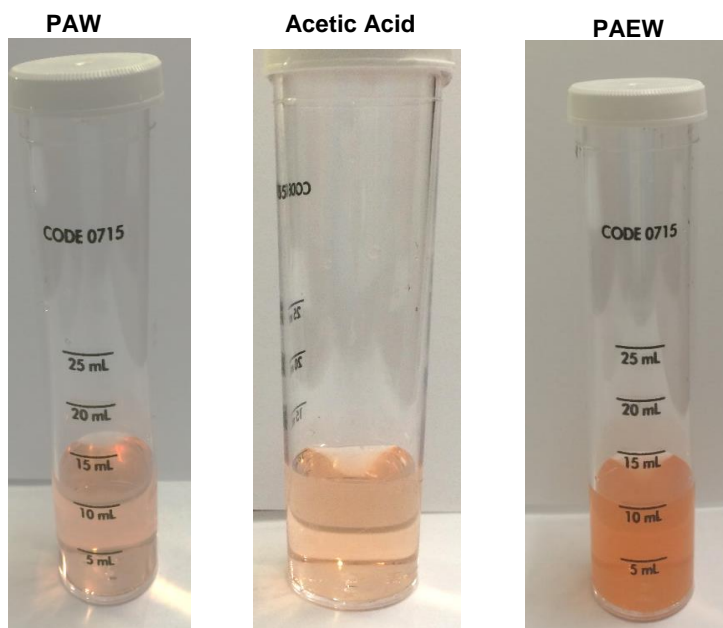


Figure 31: Peracetic acid detection using Lamotte test kit using DPD method. The test gave positive results for PAEW indicating the presence of peracetic acid.

6 SPORICIDAL ACTION OF PLASMA ACTIVATED ETHANOL WATER SOLUTION

Microorganisms sense and respond to changes in environment. Certain types of Gram-positive bacteria species such as certain *Bacillus* and *Clostridium* species form endospores when encountering environmental stress such as nutrient starvation [41] as shown in Fig 31. The bacterial spores differ significantly from the corresponding vegetative cells. Spores are metabolically dormant and exhibit resistance properties making them highly resistant to many treatments including extremes of temperature, radiation and chemical biocides [41] .

The endospores consist of many layers, in some an additional layer called exosporium is also present as shown in Figure 32. The exosporium is a thin delicate covering surrounding the spore. The spore coat lies beneath the exosporium. It is composed of several protein layers. It is impermeable and responsible for the spore's resistance to chemicals. The cortex which occupies half of the spore volume. It is filled with peptidoglycans but loosely cross linked. The next layer is the inner membrane wall which surrounds the core. The core is the cellular material containing, DNA, ribosomes and other cellular components which are in a metabolically inactive state.

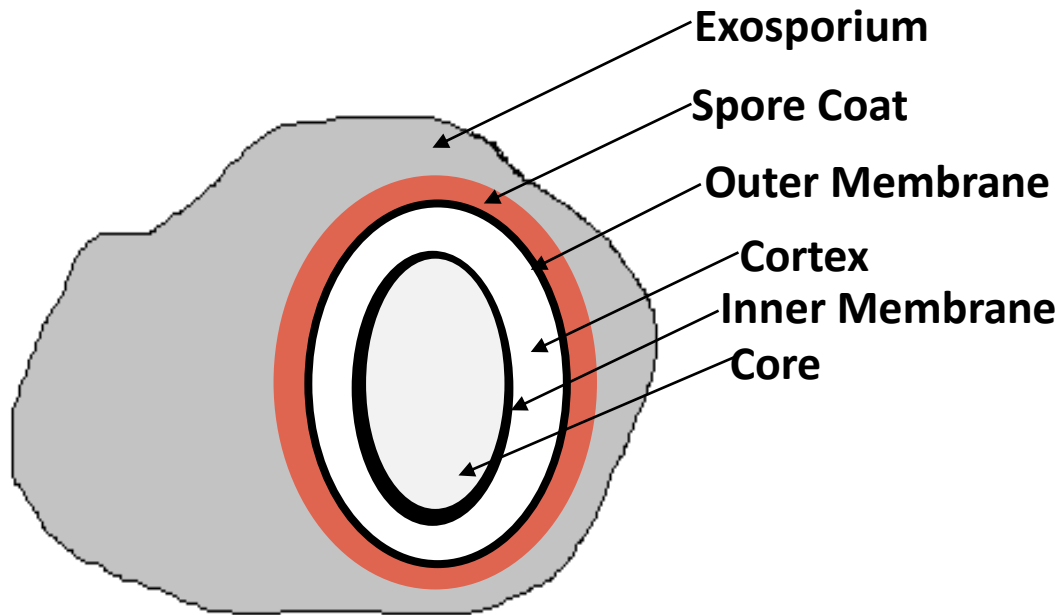


Figure 32: Endospore structure of the spore forming bacteria.

Spores are killed by a number of different ways including damage to spore's DNA, inner membrane, proteins in the core and number of different mechanisms [42]. There are many factors that contribute to resistance of spores against chemicals [43].

The plasma activation of ethanol water was found to be an effective way to kill the endospores as discussed in section 1.3. The most probable route based on the results is the hydration of spores followed by the action of peracetic acid and other species at

the inner membrane. It has been shown that spore coat is the major barrier and offers great resistant to the sporicidal action of peracetic acid [41, 44]. In the presence of water, spores swell up in minutes and start to germinate [45, 46]. The germination process with the loss of encapsulation makes them vulnerable to the environment and they won't survive without nutrients or in the presence of biocides. Water causes swelling and cracks the spore coat leading to the formation of channel like passages for peracetic acid and other species to reach the vulnerable inner parts. The peracetic acid sporicidal action is mainly due to its action at the spore's inner membrane [47]. There might be many other possible routes for the sporicidal action but a more detailed insight into the sporicidal activity is beyond the scope of this study. It should be noted that PAW also has sporicidal activity due to the presence of peroxyntrous acid and peroxyntric acid. However, the sporicidal action of PAEW is enhanced by peracetic acid which is produced in addition to above species.

7 CONCLUSIONS AND FUTURE WORK

7.1 Conclusion

The plasma activation of 35% w/w ethanol water mixture for bio medical applications is investigated. A dielectric barrier discharge setup is used to generate ambient air plasma. The input power and frequency is kept constant to mimic the initial conditions for maximum sporicidal efficiency as observed by researchers at EP Technologies, LLC. It is observed that plasma activation results in the formation of volatile species. Two new chemical compounds acetic acid and peracetic acid are found to be formed after plasma activation of the mixture in addition to the compounds such as nitrous acid, nitric acid and hydrogen peroxide formed in plasma activated water. A possible route for the sporicidal action of peracetic acid is mentioned.

7.2 Summary of Results

7.2.1 Mass vs Time Results

Mass vs time trials indicate the formation of volatile species after plasma treatment. The presence of volatile species is significant up to 9 minutes as confirmed by statistical analysis. The mass loss due to the evaporation of new species and ethanol from the mixture after plasma activation is found to be around 1% of the total mass for a

post discharge time of 20 minutes. The concentration of volatile species is found to increase with increase in activation time, power and initial temperature. However, variation of ethanol concentration in the mixture doesn't seem to have a significant effect on the formation of new species and mass vs time trials.

7.2.2 pH Trials

pH is one of the critical factors that can induce anti-bacterial effects in solutions. Most microorganisms have a critical pH of 4.7 below which it is difficult to survive. pH of both DI water and 35% ethanol water showed a similar decrease after plasma treatment from around 5.4 to 2.8 indicating that there are other factors responsible for the increased sporicidal activity of plasma activated ethanol water solution. The total concentration of plasma synthesized species in solution is estimated based on the decrease in pH and it is found to be around 1000 ppm.

7.2.3 Qualitative Analysis

Spectroscopic analysis and Gas Chromatography Mass Spectrometry tests were done to identify the new species formed in ethanol water solution after plasma treatment. The UV-Vis-NIR spectroscopic trials indicated the possible formation of acetic acid and peracetic acid after plasma treatment. The GCMS trials indicated the formation of acetic acid at m/z 60 after treatment. Various species such as nitrite, nitrate and hydrogen

peroxide which are formed during plasma activation of DI water is also detected using these tests. However, these tests could not identify the exact concentration of new species formed after plasma treatment. The possible chemical species in PAEW are summarized in Figure 33. The new species in PAEW that is formed in addition to the species formed in PAW are highlighted.

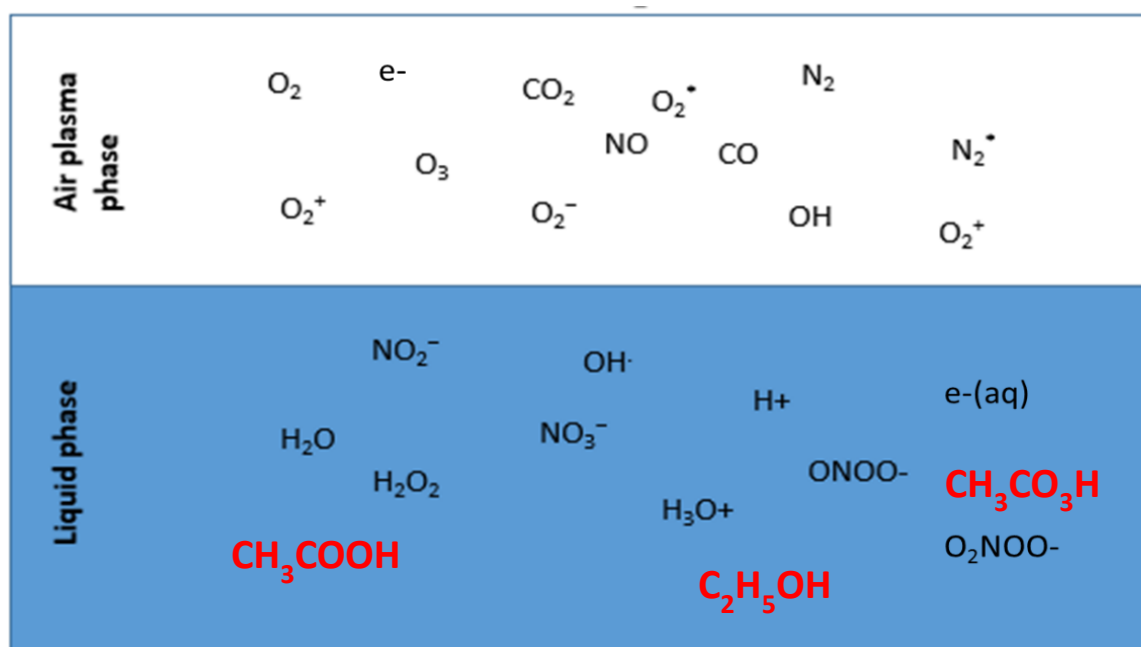


Figure 33: Possible reactive species in PAEW.

7.2.4 Quantitative Analysis

Various colorimetric and enzymatic assay tests were done to identify the concentration of nitrite, nitrate, hydrogen peroxide, acetic acid and peracetic acid which are formed during plasma treatment as indicated by the qualitative tests. The interferences from other species while testing for a particular species are taken into account. The results of the colorimetric and enzymatic assay tests are summarized in Table 3.

Table 3: Quantitative analysis results

Chemical Species	PAW	PAEW
Nitrite	50- 100 ppm	50- 100 ppm
Nitrate	100-200 ppm	100-200 ppm
Hydrogen Peroxide	200 ppm	200 ppm
Acetic Acid	NA	90-300 ppm
Peracetic Acid	NA	~200 ppm

7.2.5 Sporicidal Action

One of the possible routes of sporicidal activity of peracetic acid is studied. The spore coat is the most resistive element for the action of peracetic acid. The spore coat is destroyed by the hydration of spores which allows peracetic acid and other species to

reach the inner spore membrane and kill the spore. There might be many possible routes for the sporicidal activity that is beyond the scope of this study.

7.3 Future Work

1. *Variation with concentration* - We have seen the effects of plasma activation of 35% w/w ethanol water solution. The experiments can be repeated for different concentrations to have a better understanding of the effects of ethanol concentration.
2. *Reactor design changes* – The present DBD setup has a capability only to treat a maximum volume of 0.6ml solution. The reactor design can be changed significantly to generate more volume of liquid that can be used on a commercial scale.
3. *Investigation of Sporicidal Action* – A possible method for the observed sporicidal action is proposed. However detailed investigation using Transmission electron microscopy (TEM) image of endospores by using PAEW solution can be used to precisely identify the sporicidal activity.
4. *Investigation of air phase chemistry* – In this thesis, liquid phase chemistry is investigated in detail. However most of the air phase chemistry is obtained from literature studies. Air phase chemistry can be studied in more detail by using techniques such as optical emission spectroscopy to study the discharge conditions in more detail.

REFERENCES

1. Agency for Healthcare Research and Quality: *AHRQ's efforts to prevent and reduce healthcare-associated infections. Document 09-P013HAI_HAI 11/17/10. Available at: <http://www.ahrq.gov/qual/haiflyer.pdf>.*
2. Zimlichman, E., D. Henderson, O. Tamir, C. Franz, P. Song, C.K. Yamin, C. Keohane, C.R. Denham, and D.W. Bates, *Health care-associated infections: a meta-analysis of costs and financial impact on the US health care system. JAMA Internal Medicine*, 2013. **173**(22): p. 2039-2046.
3. Jablonowski, H. and T. von Woedtke, *Research on plasma medicine-relevant plasma-liquid interaction: What happened in the past five years? Clinical Plasma Medicine*, 2015. **3**(2): p. 42-52.
4. Yang, Y., A.V. Bazhin, J. Werner, and S. Karakhanova, *Reactive oxygen species in the immune system. International Reviews of Immunology*, 2013. **32**(3): p. 249-270.
5. Malik, M.A., A. Ghaffar, and S.A. Malik, *Water purification by electrical discharges. Plasma Sources Science and Technology*, 2001. **10**(1): p. 82.
6. Mariotti, D., J. Patel, V. Švrček, and P. Maguire, *Plasma-liquid interactions at atmospheric pressure for nanomaterials synthesis and surface engineering. Plasma Processes and Polymers*, 2012. **9**(11-12): p. 1074-1085.

7. Fridman, G., G. Friedman, A. Gutsol, A.B. Shekhter, V.N. Vasilets, and A. Fridman, *Applied plasma medicine*. Plasma Processes and Polymers, 2008. **5**(6): p. 503-533.
8. Laroussi, M., *Low-temperature plasmas for medicine?* IEEE Transactions on Plasma Science, 2009. **37**(6): p. 714-725.
9. Sears, J., S. Mohades, H. Razavi, and M. Laroussi, *Measurement of hydrogen peroxide concentrations in plasma activated media*. 22nd International Symposium on Plasma Chemistry, Antwerp, Belgium.
10. Kojtari, A., U.K. Ercan, J. Smith, G. Friedman, R.B. Sensenig, S. Tyagi, S.G. Joshi, H.-F. Ji, and A.D. Brooks, *Chemistry for antimicrobial properties of water treated with non-equilibrium plasma*. Journal of Nanomedicine & Biotherapeutic Discovery, 2014. **2014**.
11. Chu, P.K. and X. Lu, *Low temperature plasma technology: Methods and applications*. 2013: CRC Press.
12. Kong, M.G., G. Kroesen, G. Morfill, T. Nosenko, T. Shimizu, J. Van Dijk, and J. Zimmermann, *Plasma medicine: an introductory review*. New Journal of Physics, 2009. **11**(11): p. 115012.
13. Eliasson, B. and U. Kogelschatz, *Modeling and applications of silent discharge plasmas*. IEEE Transactions on Plasma Science, 1991. **19**(2): p. 309-323.
14. Kogelschatz, U., B. Eliasson, and M. Hirth, *Ozone generation from oxygen and air: discharge physics and reaction mechanisms*. 1988.
15. Fridman, A., *Plasma chemistry*. 2008: Cambridge University Press.

16. Lieberman, M.A. and A.J. Lichtenberg, *Principles of plasma discharges and materials processing*. 2005: John Wiley & Sons.
17. Fridman, G., A.D. Brooks, M. Balasubramanian, A. Fridman, A. Gutsol, V.N. Vasilets, H. Ayan, and G. Friedman, *Comparison of direct and indirect effects of non-thermal atmospheric-pressure plasma on bacteria*. Plasma Processes and Polymers, 2007. **4**(4): p. 370-375.
18. Machala, Z., B. Tarabova, K. Hensel, E. Spetlikova, L. Sikurova, and P. Lukes, *Formation of ROS and RNS in Water Electro-Sprayed through Transient Spark Discharge in Air and their Bactericidal Effects*. Plasma Processes and Polymers, 2013. **10**(7): p. 649-659.
19. Van Gils, C., S. Hofmann, B. Boekema, R. Brandenburg, and P. Bruggeman, *Mechanisms of bacterial inactivation in the liquid phase induced by a remote RF cold atmospheric pressure plasma jet*. Journal of Physics D: Applied Physics, 2013. **46**(17): p. 175203.
20. Julák, J., V. Scholtz, S. Kotúčová, and O. Janoušková, *The persistent microbicidal effect in water exposed to the corona discharge*. Physica Medica, 2012. **28**(3): p. 230-239.
21. Burlica, R., R. Grim, K.Y. Shih, D. Balkwill, and B. Locke, *Bacteria inactivation using low power pulsed gliding arc discharges with water spray*. Plasma Processes and Polymers, 2010. **7**(8): p. 640-649.

22. Kogelschatz, U., *Dielectric-barrier discharges: their history, discharge physics, and industrial applications*. Plasma Chemistry and Plasma Processing, 2003. **23**(1): p. 1-46.
23. Fridman, A. and L.A. Kennedy, *Plasma physics and engineering*. 2004: CRC Press.
24. Leduc, M., S. Coulombe, and R.L. Leask, *Atmospheric pressure plasma jet deposition of patterned polymer films for cell culture applications*. IEEE Transactions on Plasma Science, 2009. **37**(6): p. 927-933.
25. Brisset, J.-L., B. Benstaali, D. Moussa, J. Fanmoe, and E. Njoyim-Tamungang, *Acidity control of plasma-chemical oxidation: applications to dye removal, urban waste abatement and microbial inactivation*. Plasma Sources Science and Technology, 2011. **20**(3): p. 034021.
26. Brisset, J.-L. and J. Pawlat, *Chemical effects of air plasma species on aqueous solutes in direct and delayed exposure modes: discharge, post-discharge and plasma activated water*. Plasma Chemistry and Plasma Processing, 2016. **36**(2): p. 355-381.
27. Robinson, K.M. and J.S. Beckman, *Synthesis of peroxyxynitrite from nitrite and hydrogen peroxide*. Methods in Enzymology, 2005. **396**: p. 207-214.
28. Ikawa, S., A. Tani, Y. Nakashima, and K. Kitano, *Physicochemical properties of bactericidal plasma-treated water*. Journal of Physics D: Applied Physics, 2016. **49**(42): p. 425401.

29. Oehmigen, K., J. Winter, M. Hähnel, C. Wilke, R. Brandenburg, K.D. Weltmann, and T. von Woedtke, *Estimation of possible mechanisms of Escherichia coli inactivation by plasma treated sodium chloride solution*. Plasma Processes and Polymers, 2011. **8**(10): p. 904-913.
30. Lessa, F.C., Y. Mu, W.M. Bamberg, Z.G. Beldavs, G.K. Dumyati, J.R. Dunn, M.M. Farley, S.M. Holzbauer, J.I. Meek, and E.C. Phipps, *Burden of Clostridium difficile infection in the United States*. New England Journal of Medicine, 2015. **372**(9): p. 825-834.
31. Nerandzic, M.M., V.C. Sunkesula, P. Setlow, and C.J. Donskey, *Unlocking the sporicidal potential of ethanol: induced sporicidal activity of ethanol against Clostridium difficile and Bacillus spores under altered physical and chemical conditions*. PloS One, 2015. **10**(7): p. e0132805.
32. Ikawa, S., K. Kitano, and S. Hamaguchi, *Effects of pH on Bacterial Inactivation in Aqueous Solutions due to Low-Temperature Atmospheric Pressure Plasma Application*. Plasma Processes and Polymers, 2010. **7**(1): p. 33-42.
33. Orlando, J.J. and G.S. Tyndall, *Gas phase UV absorption spectra for peracetic acid, and for acetic acid monomers and dimers*. Journal of Photochemistry and Photobiology A: Chemistry, 2003. **157**(2): p. 161-166.
34. McConnell, J.S., R. McConnell, and L. Hossner. *Ultraviolet spectra of acetic acid, glycine, and glyphosate*. in Proceedings Arkansas Academy of Science. 1993.

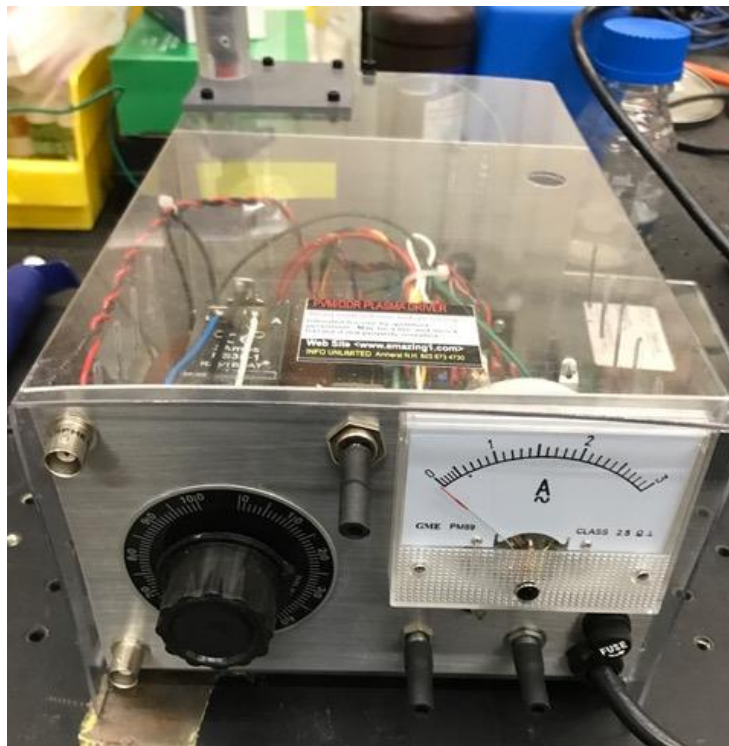
35. Friedel, R., J. Shultz, and A. Sharkey, *Mass spectrum of nitric acid*. Analytical Chemistry, 1959. **31**(6): p. 1128-1128.
36. Linstrom, P.J. and W. Mallard, *NIST Chemistry webbook; NIST standard reference database No. 69*. 2001.
37. Read, D.M., *Hydrogen peroxide and peracetic acid indicators and methods using the same*. 2004, Google Patents.
38. Klenk, H., P.H. Götz, R. Siegmeier, and W. Mayr, *Peroxy compounds, organic*. Ullmann's Encyclopedia of Industrial Chemistry, 2000.
39. Putt, K.S. and R.B. Pugh, *A high-throughput microtiter plate based method for the determination of peracetic acid and hydrogen peroxide*. PloS one, 2013. **8**(11): p. e79218.
40. Marquis, R., G. Rutherford, M. Faraci, and S. Shin, *Sporicidal action of peracetic acid and protective effects of transition metal ions*. Journal of industrial Microbiology, 1995. **15**(6): p. 486-492.
41. Leggett, M.J., J.S. Schwarz, P.A. Burke, G. McDonnell, S.P. Denyer, and J.-Y. Maillard, *Resistance to and killing by the sporicidal microbicide peracetic acid*. Journal of Antimicrobial Chemotherapy, 2015. **70**(3): p. 773-779.
42. Setlow, P., *Spore resistance properties*. Microbiology spectrum, 2014. **2**(5).
43. Setlow, P., *Spores of Bacillus subtilis: their resistance to and killing by radiation, heat and chemicals*. Journal of Applied Microbiology, 2006. **101**(3): p. 514-525.
44. Driks, A., *Bacillus subtilis spore coat*. Microbiology and Molecular Biology Reviews, 1999. **63**(1): p. 1-20.

45. Driks, A., *The dynamic spore*. Proceedings of the National Academy of Sciences, 2003. **100**(6): p. 3007-3009.
46. Sahin, O., E.H. Yong, A. Driks, and L. Mahadevan, *Physical basis for the adaptive flexibility of Bacillus spore coats*. Journal of The Royal Society Interface, 2012. **9**(76): p. 3156-3160.
47. Leggett, M.J., J.S. Schwarz, P.A. Burke, G. McDonnell, S.P. Denyer, and J.-Y. Maillard, *Mechanism of sporicidal activity for the synergistic combination of peracetic acid and hydrogen peroxide*. Applied and Environmental Microbiology, 2016. **82**(4): p. 1035-1039.

APPENDIX A

Instruments Used and their specifications

- 1) Power Supply- To generate Dielectric Barrier discharge



- Amazing 1 PVM 500
- High Voltage High Frequency power supply
- Power type : AC
- Voltage range: 0 – 30 kV peak to peak
- Frequency range: 20 kHz to 70 kHz
- Output power : 10 to 200 W

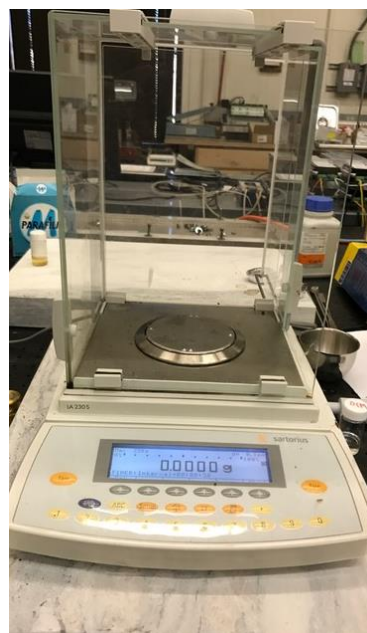
2) Power meter- To monitor power input to reactor

- Kill A Watt Power meter
- 0.2% Accuracy
- Operating Voltage – 115VAC
- Can monitor voltage, current etc.



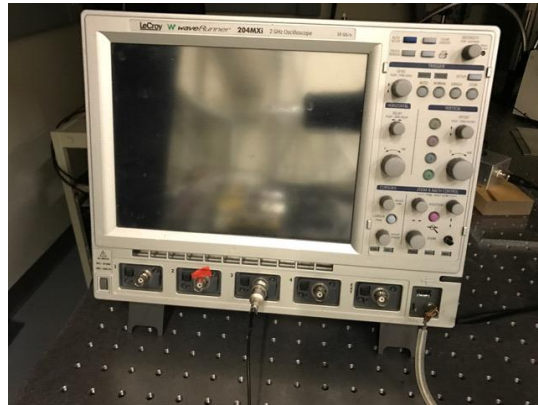
3) Mass balance- To make precision mass measurements

- Sartorius LA 230S Mass Balance
- Readability - 0.1 mg
- Weighing capacity - 120 g
- Response time (avg.) ≤ 2 sec
- Repeatability $\leq \pm 0.1$ mg
- Linearity $\leq \pm 0.2$ mg



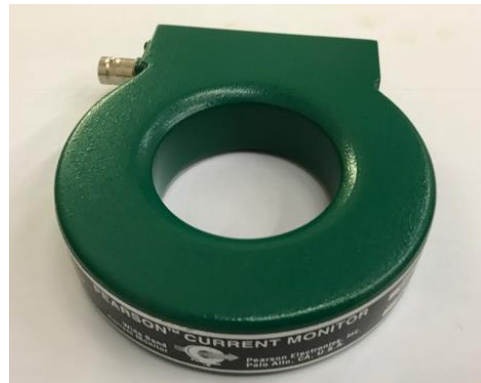
4) Oscilloscope – To monitor output voltage and current waveforms

- Lecroy Waverunner 204mxi Oscilloscope
- Bandwidth – 2 GHz
- Input Channels -4
- Sample Rate- 5 GSa/sec
- Memory depth – 12.5 Mpts/Ch



5) Current Transformer

- Pearson Current Monitor Model no 6585
- Sensitivity – 1V/A
- Maximum peak current – 500 A
- Output resistance – 50 ohm



6) Voltage probe

- PMK 14KV AC
- Max Voltage- 20KV
- Max Frequency – 100 MHZ



7)UV-Vis NIR Spectrophotometer

- U-4100 UV-Vis-NIR Spectrophotometer
- Double beam spectrophotometer
- Wavelength range- 185 to 3300 nm
- Cell – 10 mm path length quartz
- Used for both solid/liquid samples



8)FTIR Spectroscope

- Thermo Nicolet 380 FTIR Spectroscope
- Spectral range – 7800 to 350 cm^{-1}
- Used for both ATR spectra and Transmittance spectra



9)GCMS

- Ultra GC/DSQ (ThermoElectron, Waltham, MA)
- Electron impact ionization (EI) and Chemical Ionization techniques
- Column- Rxi-5ms (60 m length, 0.25 mm ID and 0.25 μm film thickness.)
- Carrier gas - Helium
- Injection Volume - 1 μL .
- Split/ Splitless injection technique



APPENDIX B

1) SAS Code

Statistical analysis was done on the data from the 20 trials for untreated sample and 25 trials for the treated sample to identify if there is any statistically significant difference between treated and untreated samples. The t-test for 2 samples was done for the untreated and treated values for different times using SAS 9.8 software for a 95% confidence interval.

```
data response;
    input group $ mass;
    datalines;
C      0.018753447
C      0.01920966
C      0.019769357
C      0.019199122
C      0.018302829
C      0.018259936
C      0.018398268
C      0.02039627
C      0.022129187
C      0.018591549
C      0.020547945
C      0.015168539
C      0.013274336
C      0.017665953
C      0.015965939
C      0.016505407
C      0.018082192
C      0.016901408
C      0.017553191
t      0.021799888
t      0.022096317
t      0.020821609
t      0.021082621
t      0.020536224
t      0.020624303
t      0.027972028
t      0.024375743
t      0.02084507
t      0.029395138
```

```

t      0.022075055
t      0.018240343
t      0.019764957
t      0.022407504
t      0.021540118
t      0.0202407
t      0.020218579
t      0.017003188
t      0.027991218
;
proc univariate data=response normal plot;
    class group;
    var mass;
histogram mass/ midpoints = 0.013 to 0.03 by 0.005 normal;
run;
proc ttest data= response;
    title 'Two sample t test';
    class group;
    var mass;
run;

```

2) MATLAB Code for calculating average power in a cycle.

```

V=dlmread('C:\Users\josef\Documents\Josef\Project EP
technologies\7.Fall2016\Thesis\Discharge VI
Characteristics\C2EtOH_C220kV_C3Pearson00000.dat');
I=dlmread('C:\Users\josef\Documents\Josef\Project EP
technologies\7.Fall2016\Thesis\Discharge VI
Characteristics\C3EtOH_C220kV_C3Pearson00000.dat');
P=V(:,2).*I(:,2);del_t=V(2,1)-V(1,1)
figure
plot(V(:,1),P)
figure,plot(V(:,1),V(:,2)),yyaxis right,plot(I(:,1),I(:,2))
ilow=find(V(:,2)>0,1,'first')
ihigh=find(V(:,2)<0,1,'last')
V2=V(ilow:ihigh,:);
I2=I(ilow:ihigh,:);
P=V2(:,2).*I2(:,2);
yNew=cumtrapz(P(:))*del_t;
plot(V2(:,1),yNew);
plot(V2(:,1),yNew);
figure,plot(V2(:,1),V2(:,2)),yyaxis right,plot(I2(:,1),I2(:,2));
yNew(end)*23000/5;

```

APPENDIX C

1)pH Test calculations

The pH of ethanol water mixture was found to decrease from 5.4 to 2.8 after plasma concentration. The strong nitric acid HNO_3 will be fully ionized and we take nitric acid as a reference in our calculations.

Concentration of H^+ in 0.6 ml of ethanol water solution before plasma activation,

$$[\text{H}^+] = 10^{-\text{pH}} = 10^{-5.4} = 3.98 * 10^{-6} \text{ M}$$

Concentration of H^+ in 0.6 ml of ethanol water solution after plasma activation,

$$[\text{H}^+] = 10^{-\text{pH}} = 10^{-2.8} = 1.58 * 10^{-3} \text{ M}$$

Concentration of HNO_3 after plasma treatment= $1.58 * 10^{-3} \text{ M} - 3.98 * 10^{-6} \text{ M}$

$$= 1.576 * 10^{-3} \text{ M}$$

Concentration of HNO_3 in ppm = $1.576 * 10^{-3} * 63 * 1000 \text{ mg/L} = 100 \text{ ppm}$

2)Energy Estimates of Species generation

Power Input, $P = 13 \text{ W}$

Plasma activation time, $t = 60 \text{ seconds}$

Energy Input, $E_i = P * t$

$$E_i = 780 \text{ J}$$

Density of 35% ethanol water solution, $d = 0.945 \text{ g/ml}$

Percentage weight of new species formed after plasma treatment, $p = 0.1\% (1000 \text{ ppm})$

Mass of new species formed in 0.6ml of 35% Et OH solution, $m = p * v * d$

$$m = 0.567 \text{ g}$$

Energy input per kg of new species, $E_{in} = E_i / m$

$$E_{in} = 1376 \text{ kJ/kg}$$

Heat of formation of HNO_3 , $h_f = 207 \text{ kJ/mol} = 207/63 \text{ kJ/kg} = 3.28 \text{ kJ/kg}$

Electrical energy to chemical energy conversion efficiency, $\eta = E_{in}/h_f * 100$

$$\eta = 0.23\%$$

3)Finger print locations and width for UV-Vis-NIR Spectroscopy

Table C.1: Finger print region peak locations and width

Peak Location (nm)	Peak Width (nm)	Peak Location (nm)	Peak Width (nm)	Peak Location (nm)	Peak Width (nm)
2694.5	3.5	3085.5	5.5	3200	4.5
2706	8.5	3100.5	3.5	3206	2.5
2716.5	5.5	3120	0.5	3222	0.5
2724	0.5	3132	0.5	3229.5	7.5
2726.5	1.5	3142	2.5	3237	2.5
2734.5	5.5	3151.5	1.5	3247.5	1.5
2750	22.5	3159.5	7.5	3251	2.5
2765	2.5	3166.5	1.5	3254	0.5
2775	2.5	3175.5	5.5	3264	2.5
2786	4.5	3185	2.5	3282.5	7.5
		3195.5	1.5	3293.5	7.5

APPENDIX D

Colorimetric and Enzymatic Assays

1) Hydrogen Peroxide VACUettes Visual High Range Kit



- Double beam spectrophotometer
- Ferric Thiocyanate method
- Range – 0 to 1200 ppm
- Possible interference from peracetic acid

2) Seachem Multitest Nitrite and Nitrate detection kit



- Separate tests for nitrite and nitrate detection
- Detection limit of Nitrite $< 0.1 \text{ mg/L}$
- Detection limit of Nitrate $< 0.2 \text{ mg/L}$

3) Lamotte Hydrogen peroxide and peracetic acid detection kit



- Specific for acetic acid
- Manual format UV method
- Reaction time $\sim 4\text{min}$
- Detection limit – 0.063mg/L

4) Megazyme K-ACETRM Enzymatic Assay Kit



- Separate tests for hydrogen peroxide and peracetic acid
- Sensitivity – 50 ppm for H_2O_2
- Sensitivity – 15 ppm for PAA

APPENDIX E

Principle of Megazyme K-ACETRM Assay

(1) Acetate kinase (AK) in the presence of ATP converts acetic acid (acetate) into acetyl-phosphate and adenosine-5'-diphosphate (ADP)



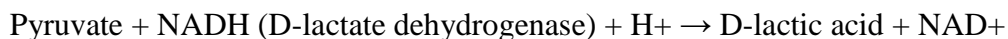
(2) This reaction is significantly accelerated by the rapid conversion of the acetyl-phosphate product into acetyl-CoA and inorganic phosphate, by the action of phosphotransacetylase (PTA) in the presence of coenzyme A (CoA)



(3) The ADP formed in (1) is reconverted into ATP and pyruvate, by phosphoenolpyruvate (PEP) in the presence of pyruvate kinase (PK).



(4) In the presence of the enzyme D-lactate dehydrogenase (D-LDH), pyruvate is reduced to D-lactate by reduced nicotinamide-adenine dinucleotide (NADH) with the production of NAD⁺.



The amount of NAD⁺ formed in the above reaction pathway is stoichiometric with the amount of Acetic Acid. It is the NADH consumption which is measured by the decrease in absorbance at 340 nm.